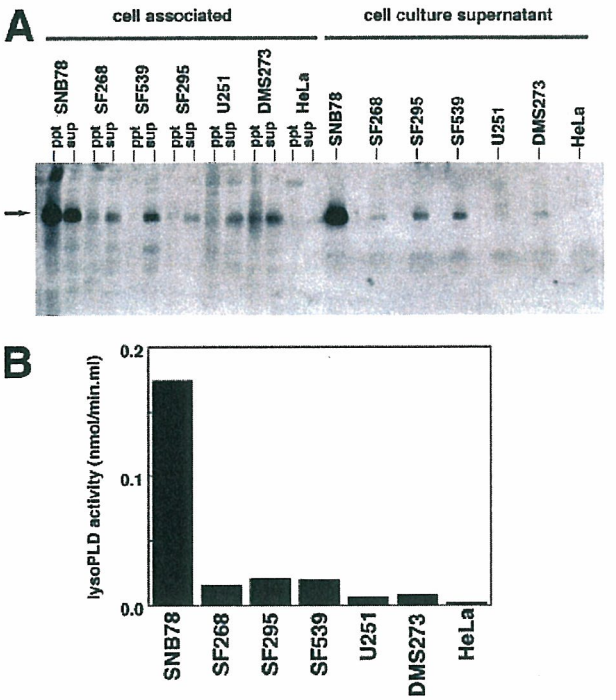

FIGURE 2. **ATX protein and lysoPLD activity in glioblastoma cell lines.** *A*, Western blot of cell membrane fractions (*ppt*), soluble fraction (*sup*), and cell culture medium using anti-human ATX monoclonal antibody 3D1. *B*, lysoPLD activity of culture media from glioblastoma and other cancer cell lines. LPC was used as the substrate.

cultured in serum-free RPMI 1640 containing 0.1% fatty acid-free bovine serum albumin (Sigma) for 2 days. LPC was extracted from culture media using the Bligh and Dyer method (51) and resuspended in phosphate-buffered saline containing 0.1% bovine serum albumin. LPC concentration was determined by a recently developed enzymatic colorimetric method as described. Briefly, samples were treated with lysophospholipase, glycerophosphorylcholine, phosphodiesterase, and choline oxidase. The resulting hydrogen peroxide generated was quantified using horseradish peroxidase and TOOS reagent.

RNA Interference—SNB-78 glioblastoma cells were transfected with siRNA oligonucleotide duplexes 1 day after confluence (day −1) with trans-it TKO (Takara, Kyoto, Japan) according to the manufacturer's instructions. Generally 20 nM siRNA was transfected with 0.5 μl of Lipofectamine per well of a 24-well plate with fresh media. Each experiment contained equivalent samples transfected with a non-targeting control siRNA pool and samples not treated with trans-it TKO. siRNA oligonucleotide duplexes for each gene of interest were purchased from WAKO (Osaka, Japan) as optimized single duplexes (ATX1, sense, 5′-gccguuggagucaauaucuGC-3′, antisense, 5′-agauauugacuccaacggcAA-3′ and ATX2, sense, 5′-gggagacugcuguaccaauTA-3′, antisense, 5′-auugguacagcagucucccCT-3′). Transfection efficiency was monitored using fluorescent (Cy3)-tagged oligonucleotides (Blockit, Invitrogen) transfected as described above and visualized with a mercury lamp fluorescent microscope.

RESULTS

Expression of ATX and LPA Receptors in 50 Tumor Cell Lines—We examined the expression of ATX in 50 cultured human tumor cell lines derived from various tumors using the quantitative RT-PCR technique. We found that some cells expressed a significant amount of ATX at both the mRNA and the protein levels (Figs. 1 and 2). High ATX expression was detected in DMS273 (lung cancer), colo320 (colon cancer), SKOV3

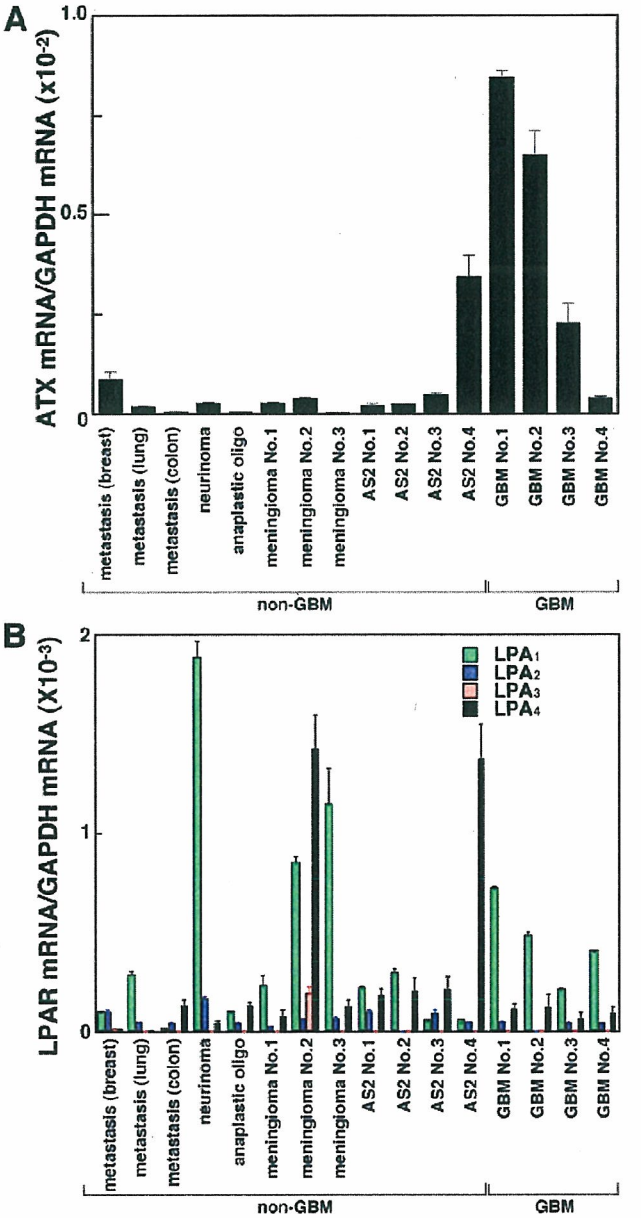

FIGURE 3. **Enhanced expression of ATX in GBM tissues.** Expressions of ATX (*A*) and LPA receptors (LPA_1, LPA_2, LPA_3, and LPA_4) (*B*) in various brain tumor tissues as measured by quantitative RT-PCR. Of the three LPA receptors (*LPAR*), LPA_1 has the highest expression in various brain tumors, possibly reflecting the high LPA_1 expression in normal human brain. Note that tissues AS2 number 4 and GBM number 1 are derived from the same patient. The patient's cancer was initially diagnosed as astrocytoma, and after the recurrence, it was diagnosed as GBM.

(ovarian cancer), MKN1 (stomach cancer), and most of the brain cancer cells (SF295, SF539, SF268, SNB-75, and SNB-78). The expression was highest in SNB-78 cells. In good agreement with this observation, both ATX protein and lysophospholipase D activity were detected in the culture supernatants of these ATX-positive cells (Fig. 2). Most of the protein was detected in the culture cell supernatants, whereas a small amount was detected in cells (Fig. 2*A*). These results confirm that ATX is secreted from cells, although ATX is initially biosynthesized in cells as a type II membrane protein.

We also examined the expression of the LPA receptors (LPA_1, LPA_2, LPA_3, and LPA_4) in the 50 human tumor cell lines using quantitative

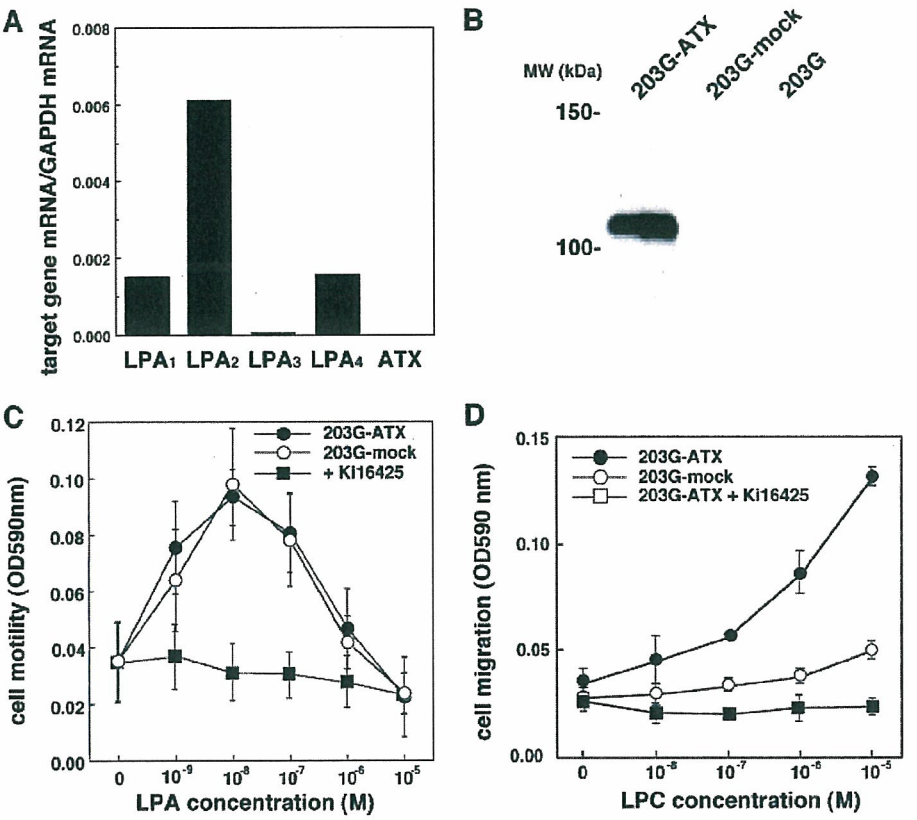

FIGURE 4. **Overexpression of ATX in combination with LPC induces a migratory response in glioma cells in Boyden chamber assay.** *A*, expression profiles of LPA receptors (LPA_1, LPA_2, LPA_3, and LPA_4) and ATX in mouse glioma cell line 203g as measured by quantitative RT-PCR. *B*, expression of ATX in stably transfected 203g-ATX cells as measured by Western blotting. *mock*, mock-transfected; *MW*, molecular mass markers. *C*, migratory responses of 203g-ATX (*closed circles*) and mock-transfected cells (*open circles*) to LPA and the effect of LPA_1 antagonist, Ki16425, on the migratory response (*closed squares*). *D*, migratory responses of 203g-ATX cells (*closed circles*) and mock-transfected cells (*open circles*) to LPC and the effect of Ki16425 on the migratory response (*closed squares*).

RT-PCR. Although the expression pattern of the four LPA receptors does not necessarily reflect the tissue origin of the tumor cells, restricted LPA receptor expression patterns were obtained (Fig. 1). LPA_2 was predominantly expressed in cells from colon, stomach, and breast cancers (36, 37). LPA_3 expression was relatively low. However, LPA_3 was expressed by certain ovarian and prostate cancer cell lines. Expression of LPA_4 was fairly low. By contrast, LPA_1 was dominant in brain tumor cells (Fig. 2).

Expression of ATX and LPA Receptors in GBM—Because SF295, SF539, SF268, SNB-75, and SNB-78 are defined as glioblastomas (gliomas derived from GBM), we attempted to examine the expression of ATX and LPA receptors in tissues from various brain tumors. We found that expression of ATX was markedly high in GBM tissues (Fig. 3). Three of four GBM tissue samples showed extremely high ATX expression. ATX expression is apparently lower in tissues from other brain tumors. One exception is a patient of astrocytoma (case AS2 number 4) whose tissue showed high ATX expression. He experienced early recurrence after only 16 months, and the tumor progressed to GBM at recurrence (case GBM number 1). Among the four LPA receptors, LPA_1 was dominantly expressed in most brain tumor tissues tested including GBM with low expression of LPA_2, LPA_3, and LPA_4, which may reflect the expression pattern in normal brain tissues (38, 39). The expression pattern of ATX and LPA receptors in GBM tissues indicates that ATX contributes to the invasive property of glioblastomas by producing LPA.

LPC Stimulates Cell Motility of ATX-expressing Cells—To test the possibility that glioblastomas acquire their high invasiveness through autocrine production of LPA by ATX, we first examined the effect of enhanced ATX expression on cell motility. We used mouse glioma cell line 203G that expressed LPA_1 (Fig. 4*A*) but not a detectable amount of ATX (Fig. 4*B*). 203G glioma cells that stably express ATX (203G-ATX) were established by transfecting ATX cDNA and by selecting neomycin-resistant clones. The established three lines expressed significant levels of ATX as judged by both lysoPLD activity (data not shown) and Western blotting (Fig. 4*B*). In addition, these cell lines showed similar expression pattern of LPA receptors to the parental 203G cells (data not shown). The effects of LPA on the motility of transfected cells and mock-transfected 203G cells in the Boyden chamber were similar (Fig. 4*C*). LPA had a similar effect on the motility of parental 203G cells (not shown). The effect of LPA on the motility of these cells was abolished by the LPA_1 antagonist, Ki16425 (Fig. 4*C*). By contrast, these cells showed quite distinct responses to LPC. LPC significantly stimulated the migration of 203G-ATX cells in Boyden chamber assay (Fig. 4*D*). However, a similar response was not induced in mock-transfected 203G cells (Fig. 4*D*) or in parental 203G cells (not shown). In addition, the stimulatory effect of LPC in 203G-ATX cells was completely abolished by the addition of Ki16425 (Fig. 4*D*), showing that LPA mediates the LPC-stimulated cell migration of the cells through LPA_1. We confirmed that platelet-derived growth factor induced similar migratory response in ATX-overexpressing, mock-transfected, and parental 203G cells (data not shown).

We further examined the role of endogenously expressed ATX in the cell motility of ATX-expressing cells, which has not been previously demonstrated so far. For this experiment, we used SNB-78, which has the highest ATX expression among the 50 tumor cell lines (Fig. 1). As shown in Fig. 5*A*, SNB-78 cells, like other LPA_1-positive cells, showed a migratory response to exogenous LPA in the Boyden chamber. LPC also stimulated the migration of SNB-78 (Fig. 5*B*). Ki16425 blocked not only the LPA-induced migratory response but also the LPC-induced migratory response (Fig. 5). This indicates that: 1) LPC is converted to LPA by the lysoPLD activity of endogenous ATX, 2) the LPA generated subse-

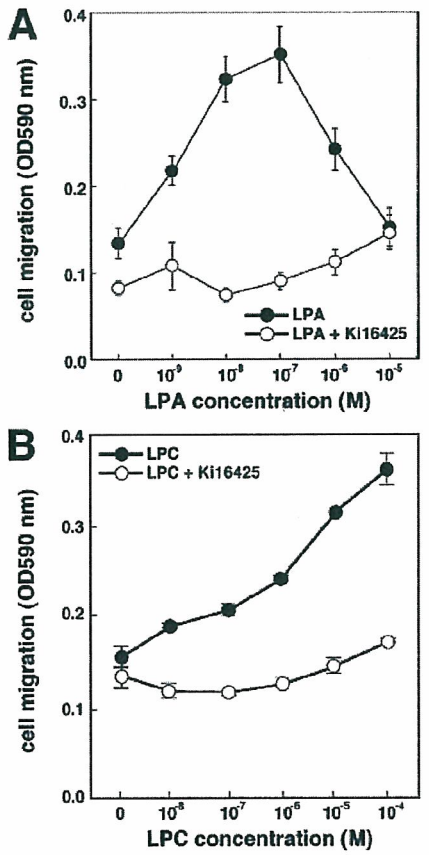

FIGURE 5. **Effects of LPA and LPC on migration of glioblastoma cells.** Migration of SNB-78 glioblastoma cells in response to LPA (*A*, *closed circles*) and LPC (*B*, *closed circles*) was measured with a Boyden chamber. Both responses were abolished by Ki16425 (*open circles*).

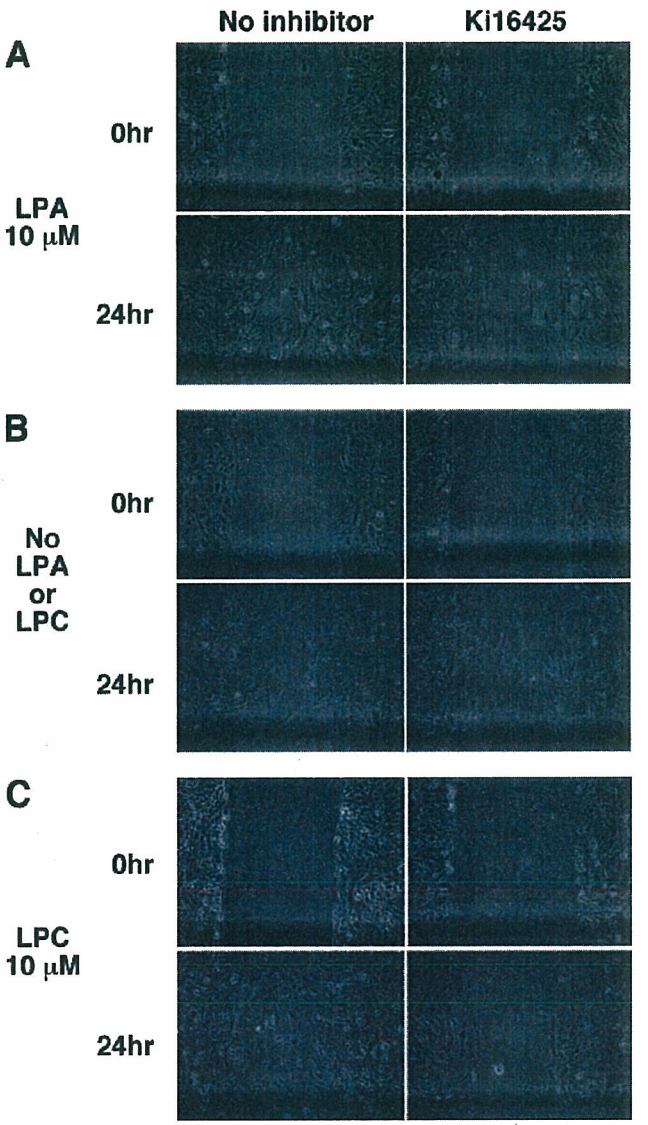

FIGURE 6. **Glioblastoma migrates in response to LPA and LPC in wound healing assay.** A clean wound area was produced on a monolayer of semiconfluent SNB-78 cells, seeded in 12-well plates. The wound was then allowed to heal for 24 h in serum-free media in the presence of LPA (10 μM, *A*) or LPC (10 μM, *C*) or in the absence of exogenous lipids (*B*). Cell morphologies before (0 h) and after (24 h) the treatment are shown in the *upper* and *lower panels*, respectively. The effect of Ki16425 (1 μM) on the cell migration is also shown in the *right panels*.

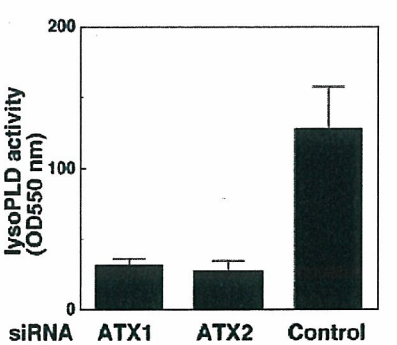

FIGURE 7. **Down-regulation of ATX in SNB-78 cells using siRNA.** One-day postconfluent SNB-78 cells were transfected with ATX (ATX1 and ATX2) or control siRNA duplexes. Forty-eight hours later, down-regulation of ATX in the cell supernatants was analyzed by measuring lysoPLD activity in the cell culture supernatant of the cells.

quently stimulates cell migration through LPA_1, and 3) LPC behaves as a chemotactic factor toward ATX-expressing cells.

We previously showed that LPC is released from cells and could be converted to LPA to induce cell migration by exogenously added ATX (14). In fact, SNB-78 was found to release a small amount of LPC into the cell culture medium, and the amount gradually increased during the culture (data not shown). However, we were unable to evaluate the effect of cell-derived LPC on cell motility in the Boyden chamber since LPC is lost during preparation of the cells for the Boyden chamber assay. Accordingly, to evaluate the effects of cell-derived LPC and ATX on cell migration, we used a wound healing assay, which takes a relatively long period. As expected, exogenously added LPA was able to induce migration of SNB-78 cells in the wound healing assay (Fig. 6*A*). The migratory response was abolished by Ki16425, which shows that LPA_1 is involved in this system, as was observed in Boyden chamber assay (Fig. 6*A*). In the absence of exogenous LPC, we observed a weak migratory response, which was also blocked by Ki16425 (Fig. 6*B*), showing that endogenous LPC and ATX, to a lesser extent, contribute to the migration of SNB-78 cells. By contrast, strong migratory responses were observed when LPC (10 μM) was added to the cells. The migratory response induced by LPC was again inhibited by Ki16425 (Fig. 6*C*). The amount of LPC released from SNB-78 was ~50 nM as judged by the enzymatic colorimetric method for determination of LPC. This indicates that the amount of endogenous LPC released from SNB-78 is insufficient to induce a full migratory response in the cells and that exogenous LPC is potentially a

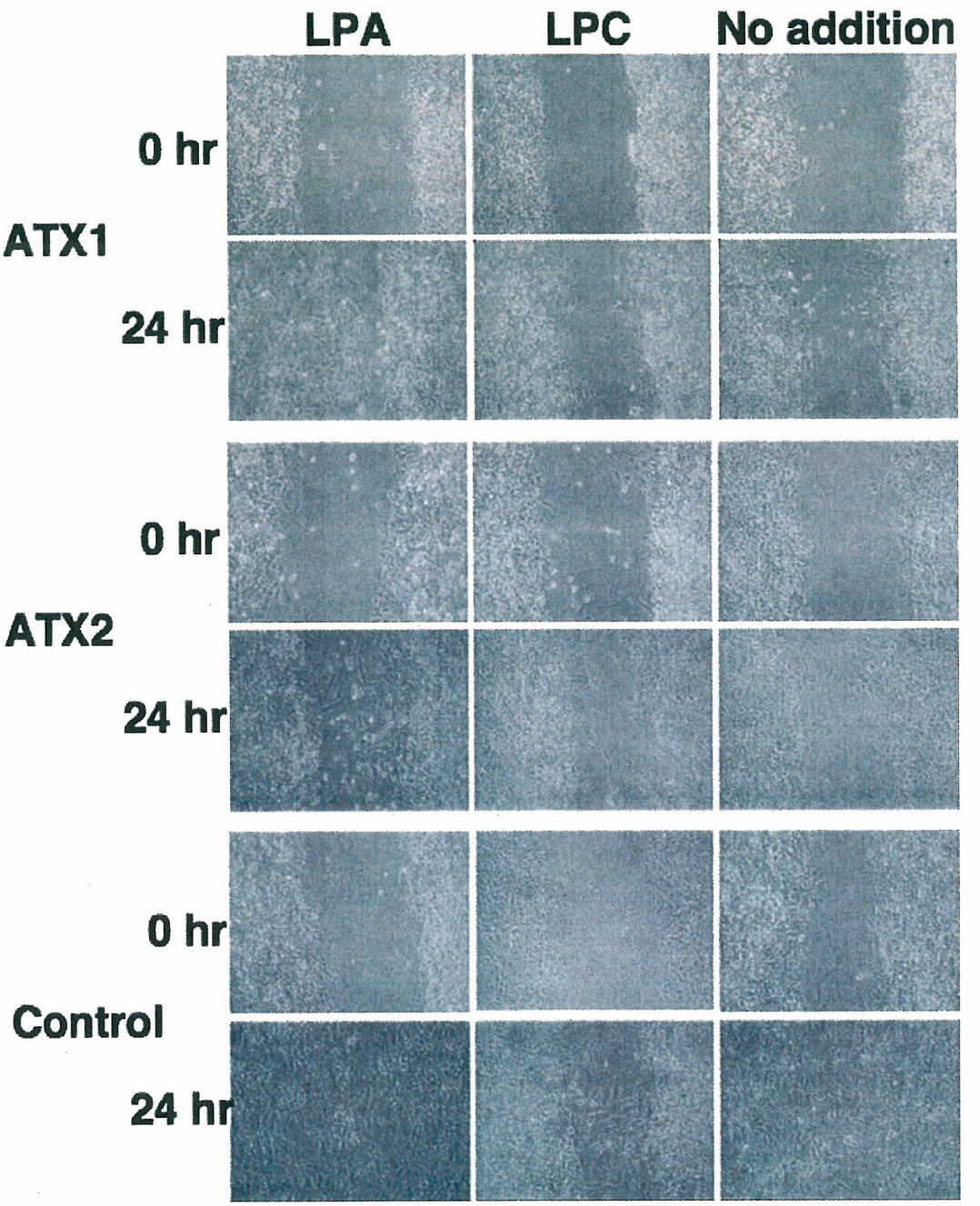

FIGURE 8. **ATX produced by SNB-78 cells contributes to the motility of the cells.** SNB-78 cells were transfected with ATX or control siRNA duplex to suppress ATX level, and after 24 h, the cells were subjected to wound healing assay both in the presence and in the absence of LPC (10 μM) for 24 h. The cells were also treated with LPA (10 μM) as a positive control. Cell morphologies before (0 h) and after (24 h) the treatment are shown in the *upper* and *lower panels*, respectively.

key factor in controlling the migratory response of ATX-expressing cells.

ATX Is Responsible for Motility of SNB-78 Cells in Wound Healing Assay—Our data suggest that endogenously expressed ATX in SNB-78 cells plays a key role in the motility of the cells by producing LPA from endogenously or exogenously supplied LPC. To confirm this hypothesis, we used siRNA to down-regulate the expression of ATX in SNB-78 cells. Confluent SNB-78 cells were transfected with varying amounts of siRNA duplexes using scramble siRNA as a control. As shown in Fig. 7, after 48 h of culture, successful down-regulation of ATX in the cell culture supernatants was confirmed by measuring lysoPLD activity of the culture cell supernatant. We next performed the wound healing assay using the ATX-down-regulated cells. We found that motility of SNB-78 cells was significantly suppressed both in the absence and in the presence of LPC, when the cells were treated with siRNA to suppress ATX expression (Fig. 8). Exogenously added LPA was able to induce migration of ATX-down-regulated cells (Fig. 8), showing that the siRNA-treated cells still retained the migratory activity in response to LPA. Thus, we concluded that ATX contributes to the cell migration of SNB-78 cells in the wound healing assay.

DISCUSSION

GBM is the most malignant brain tumor due to its high invasiveness. In this study, we found that ATX, a cell motility-stimulating factor (4), is overexpressed in GBM tissues and many glioblastoma cell lines. ATX has catalytic activity to produce a potent chemoattractant-like lipid, LPA, and stimulates cell motility through an LPA G-protein-coupled receptor, LPA_1 (14, 21). Interestingly, both GBM tissues and glioblastomas express high levels of LPA_1, and in fact, the glioblastoma, SNB-78, used in this study showed migratory responses not only to LPA but also to LPC (Figs. 5 and 6). In addition, suppression of ATX expression in SNB-78 cells by siRNA resulted in dramatic reduction of migratory response of the cells to LPC but not to LPA (Fig. 8). Furthermore, LPA_1 antagonist, Ki16425, effectively suppressed both LPA- and LPC-induced motility of glioblastoma cells. Thus, the motility of glioblastoma cells appears to depend on ATX and LPA_1. LPA-induced cell motility of glioblastomas was also shown in the previous report by Manning *et al.* (16).

Enhanced ATX expression has been repeatedly demonstrated in various tumors, including non-small cell lung cancer, breast cancer, renal cell cancer, hepatocellular carcinoma, and thyroid cancer (6–12). In breast cancer, ATX expression level strongly correlates with the invasiveness of cancer cells (8). Thus, it is reasonable to assume that ATX expressed by tumor cells is responsible for the motility, and thus, the invasiveness of the cells. However, the spontaneous motility of non-small cell lung cancer cells *in vitro* did not correlate with the levels of ATX mRNA (6), indicating that other factors may influence ATX-induced cell motility. In this study, we used glioblastoma cell lines that endogenously express ATX and cell transformants overexpressing ATX and evaluated ATX, LPA_1, and LPC, a substrate for ATX of lysoPLD activity. Our results show that LPC is a critical factor that regulates ATX-mediated cell motility. We previously showed that LPC is synthesized and released from various tumor cells and that it is a potential substrate for ATX when ATX is added to the cells in the absence of exogenous LPC (14). However, the concentration of cell-derived LPC (~50 nM) is too low to induce full cell motility of SNB-78 cells (Fig. 6). Although a high dose of exogenously added ATX induced cell motility (by converting cell-derived LPC to LPA), the amounts of endogenously expressed ATX in glioblastoma cells and even in ATX-overexpressing glioma cells were insufficient to have an effect on cell motility. We found that the addition of exogenous LPC to the ATX-expressing cells but not ATX-negative cells strongly induced cell motility, although LPA equally promoted the motility of both cell types (Figs. 4–6). Thus, LPC is a chemotactic factor for tumor cells expressing ATX and LPA_1. LPC has previously been shown to act as a chemotactic factor for other cell types, including macrophages (40), monocytes (41), and T-lymphocytes (42). In some cell types, such as macrophages, cell motility appears to be induced by another system (LPC-specific G-protein-coupled receptor, G2A) (43), whereas in other cell types, cell motility appears to be induced by the ATX-LPA_1 system.

In general, the BBB is disrupted in GBM tissue, which leads to exposure of tumor cells to components of plasma that might affect the cell motility of glioblastomas (31, 32). As indicated by Manning *et al.* (16), one such plasma component may be LPA. However, LPA concentration in plasma is quite low (below 50 nM), although in serum, it may be above 1 μM (44, 45). In contrast, LPC concentration in plasma is extremely high (100–300 μM in human and ~500 μM in rats) (35, 44). The concentration of LPC in brain tissue, such as in cerebrospinal fluids, is quite low (several μM level) (46). Thus, when the BBB is disrupted in GBM, it is likely that these tumors are exposed to LPC derived from plasma. LPC is converted to LPA by ATX expressed by glioblastomas, and consequently, LPA_1 is activated, leading to the enhanced cell motility and high invasiveness of GBM (Fig. 9). This idea is supported by the finding that GBM cells travel along blood vessels (47).

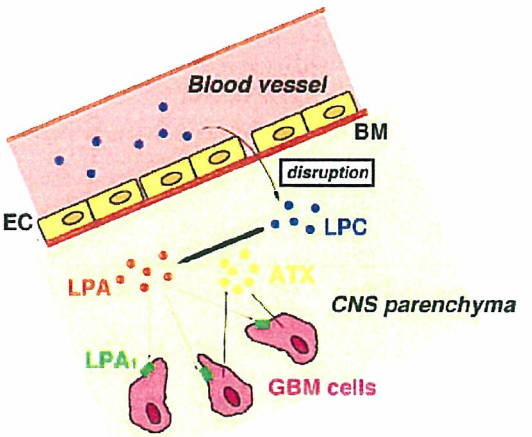

FIGURE 9. **A schematic model showing the effects of ATX, LPA_1, LPA, and LPC on the motility of GBM cells upon the disruption of BBB.** On disruption of BBB, GBM in CNS parenchyma is likely to be exposed to LPC derived from plasma. Then LPC is converted to LPA by ATX expressed by GBM and subsequently activation of LPA_1, leading to the enhanced motility and high invasiveness of GBM. *EC*, endothelial cells; *BM*, basement membrane.

The expression patterns of LPA receptors in the 50 cancer cell lines (Fig. 1) agree with the previous reports on LPA receptor expression. For example, LPA_3 expression is relatively high in cells from ovarian cancer (48) and, markedly, LPA_2 is predominantly expressed in cells derived from colon (37) and thyroid cancer (49). Recently, we also observed similar LPA receptor distribution patterns in human breast cancers (36) in which LPA_2 expression is dramatically enhanced. The present study revealed that LPA_1 is predominantly expressed in GBM cells and tissues. The same is true for ATX. Thus, the expression patterns in cancer cell lines are definitely informative to understand the roles of ATX and LPA receptors in cancer cell biology.

ATX may contribute to cancer cell survival and motility in several ways. In addition to its cell motility-stimulating activity, ATX has a cell proliferation-stimulating activity (14) and an angiogenic factor-like activity that induces new vessel formation by an unknown mechanism (50). GBM is known to induce vascular proliferation, and so ATX might have a role here as well. In summary, our results show that ATX, a potent oncogenic protein, is overexpressed in GBM and stimulates the motility of glioblastomas. Thus, ATX is a potential diagnostic marker for GBM. In addition, ATX, LPA_1 and unidentified LPC-producing enzymes are potential targets for GBM therapy.

REFERENCES

1. Stracke, M. L., Krutzsch, H. C., Unsworth, E. J., Arestad, A., Cioce, V., Schiffmann, E., and Liotta, L. A. (1992) *J. Biol. Chem.* **267,** 2524–2529
2. Goding, J. W., Terkeltaub, R., Maurice, M., Deterre, P., Sali, A., and Belli, S. I. (1998) *Immunol. Rev.* **161,** 11–26
3. Stefan, C., Gijsbers, R., Stalmans, W., and Bollen, M. (1999) *Biochim. Biophys. Acta* **1450,** 45–52
4. Stracke, M. L., Clair, T., and Liotta, L. A. (1997) *Adv. Enzyme Regul.* **37,** 135–144
5. Nam, S. W., Clair, T., Campo, C. K., Lee, H. Y., Liotta, L. A., and Stracke, M. L. (2000) *Oncogene* **19,** 241–247
6. Yang, Y., Mou, L. j., Liu, N., and Tsao, M. S. (1999) *Am. J. Respir. Cell Mol. Biol.* **21,** 216–222
7. Euer, N., Schwirzke, M., Evtimova, V., Burtscher, H., Jarsch, M., Tarin, D., and Weidle, U. H. (2002) *Anticancer Res.* **22,** 733–740
8. Yang, S. Y., Lee, J., Park, C. G., Kim, S., Hong, S., Chung, H. C., Min, S. K., Han, J. W., Lee, H. W., and Lee, H. Y. (2002) *Clin. Exp. Metastasis* **19,** 603–608

9. Stassar, M. J., Devitt, G., Brosius, M., Rinnab, L., Prang, J., Schradin, T., Simon, J., Petersen, S., Kopp, S. A., and Zoller, M. (2001) *Br. J. Cancer* **85,** 1372–1382
10. Zhao, Z., Xu, S., and Zhang, G. (1999) *Zhonghua Gan Zang Bing Za Zhi.* **7,** 140–141
11. Zhang, G., Zhao, Z., Xu, S., Ni, L., and Wang, X. (1999) *Chin. Med. J. (Engl. Ed.)* **112,** 330–332
12. Kehlen, A., Englert, N., Seifert, A., Klonisch, T., Dralle, H., Langner, J., and Hoang, V. C. (2004) *Int. J. Cancer* **109,** 833–838
13. Lee, H. Y., Clair, T., Mulvaney, P. T., Woodhouse, E. C., Aznavoorian, S., Liotta, L. A., and Stracke, M. L. (1996) *J. Biol. Chem.* **271,** 24408–24412
14. Umezu-Goto, M., Kishi, Y., Taira, A., Hama, K., Dohmae, N., Takio, K., Yamori, T., Mills, G. B., Inoue, K., Aoki, J., and Arai, H. (2002) *J. Cell Biol.* **158,** 227–233
15. Tokumura, A., Majima, E., Kariya, Y., Tominaga, K., Kogure, K., Yasuda, K., and Fukuzawa, K. (2002) *J. Biol. Chem.* **277,** 39436–39442
16. Manning, T. J., Parker, J. C., and Sontheimer, H. (2000) *Cell Motil. Cytoskeleton* **45,** 185–199
17. Sturm, A., Sudermann, T., Schulte, K. M., Goebell, H., and Dignass, A. U. (1999) *Gastroenterology* **117,** 368–377
18. Itoh, K., Yoshioka, K., Akedo, H., Uehata, M., Ishizaki, T., and Narumiya, S. (1999) *Nat. Med.* **5,** 221–225
19. Van Leeuwen, F., Olivo, C., Grivell, S., Giepmans, B. N., Collard, J. G., and Moolenaar, W. H. (2003) *J. Biol. Chem.* **278,** 400–406
20. Shida, D., Kitayama, J., Yamaguchi, H., Okaji, Y., Tsuno, N. H., Watanabe, T., Takuwa, Y., and Nagawa, H. (2003) *Cancer Res.* **63,** 1706–1711
21. Hama, K., Aoki, J., Fukaya, M., Kishi, Y., Sakai, T., Suzuki, R., Ohta, H., Yamori, T., Watanabe, M., Chun, J., and Arai, H. (2004) *J. Biol. Chem.* **279,** 17634–17639
22. Yamada, T., Sato, K., Komachi, M., Malchinkhuu, E., Tobo, M., Kimura, T., Kuwabara, A., Yanagita, Y., Ikeya, T., Tanahashi, Y., Ogawa, T., Ohwada, S., Morishita, Y., Ohta, H., Im, D. S., Tamoto, K., Tomura, H., and Okajima, F. (2004) *J. Biol. Chem.* **279,** 6595–6605
23. Tanaka, M., Kishi, Y., Takanezawa, Y., Kakehi, Y., Aoki, J., and Arai, H. (2004) *FEBS Lett.* **571,** 197–204
24. Fang, X., Gaudette, D., Furui, T., Mao, M., Estrella, V., Eder, A., Pustilnik, T., Sasagawa, T., Lapushin, R., Yu, S., Jaffe, R. B., Wiener, J. R., Erickson, J. R., and Mills, G. B. (2000) *Ann. N. Y. Acad. Sci.* **905,** 188–208
25. Fujimaki, T., Matsutani, M., Nakamura, O., Asai, A., Funada, N., Koike, M., Segawa, H., Aritake, K., Fukushima, T., Houjo, S., and *et al.* (1991) *Cancer* **67,** 1629–1634
26. Fujimaki, T. (2000) *Neurol. Med.-Chir. (Tokyo)* **40,** 1–106
27. Burger, P. C., Dubois, P. J., Schold, S. J., Smith, K. J., Odom, G. L., Crafts, D. C., and Giangaspero, F. (1983) *J. Neurosurg.* **58,** 159–169
28. Giese, A., Rief, M. D., Loo, M. A., and Berens, M. E. (1994) *Cancer Res.* **54,** 3897–3904
29. Hauglan, H., Tysnes, B., and Tysnes, O. (1997) *Anticancer Res.* **17,** 1035–1043
30. Westermarck, J., and Khri, V. (1999) *FASEB J.* **13,** 781–792
31. Wolff, M., and Boker, D.-K. (1999) *Clin. Neuropathol.* **8,** 72–78
32. Seitz, R., and Wechsler, W. (1987) *Acta Neuropathol.* **73,** 145–152
33. Yamori, T., Matsunaga, A., Sato, S., Yamazaki, K., Komi, A., Ishizu, K., Mita, I., Edatsugi, H., Matsuba, Y., Takezawa, K., Nakanishi, O., Kohno, H., Nakajima, Y., Komatsu, H., Andoh, T., and Tsuruo, T. (1999) *Cancer Res.* **59,** 4042–4049
34. Niwa, H., Yamamura, K., and Miyazaki, J. (1991) *Gene (Amst.)* **108,** 193–199
35. Kishimoto, T., Soda, Y., Matsuyama, Y., and Mizuno, K. (2002) *Clin. Biochem.* **35,** 411–416
36. Kitayama, J., Shida, D., Sako, A., Ishikawa, M., Hama, K., Aoki, J., Arai, H., and Nagawa, H. (2004) *Breast Cancer Res.* **6,** R640-R646
37. Shida, D., Watanabe, T., Aoki, J., Hama, K., Kitayama, J., Sonoda, H., Kishi, Y., Yamaguchi, H., Sasaki, S., Sako, A., Konishi, T., Arai, H., and Nagawa, H. (2004) *Lab. Investig.* **84,** 1352–1362
38. An, S., Bleu, T., Hallmark, O. G., and Goetzl, E. J. (1998) *J. Biol. Chem.* **273,** 7906–7910
39. Bandoh, K., Aoki, J., Hosono, H., Kobayashi, S., Kobayashi, T., Murakami, M. K., Tsujimoto, M., Arai, H., and Inoue, K. (1999) *J. Biol. Chem.* **274,** 27776–27785
40. Lauber, K., Bohn, E., Krober, S. M., Xiao, Y. J., Blumenthal, S. G., Lindemann, R. K., Marini, P., Wiedig, C., Zobywalski, A., Baksh, S., Xu, Y., Autenrieth, I. B., Schulze, O. K., Belka, C., Stuhler, G., and Wesselborg, S. (2003) *Cell* **113,** 717–730
41. Hoffman, R. D., Kligerman, M., Sundt, T. M., Anderson, N. D., and Shin, H. S. (1982) *Proc. Natl. Acad. Sci. U. S. A.* **79,** 3285–3289
42. Ryborg, A., Deleuran, B., Thestrup-Pedersen, K., and Kragballe, K. (1994) *Arch. Dermatol. Res.* **286,** 462–465
43. Radu, C. G., Yang, L. V., Riedinger, M., Au, M., and Witte, O. N. (2004) *Proc. Natl. Acad. Sci. U. S. A.* **101,** 245–250
44. Aoki, J., Taira, A., Takanezawa, Y., Kishi, Y., Hama, K., Kishimoto, T., Mizuno, K., Saku, K., Taguchi, R., and Arai, H. (2002) *J. Biol. Chem.* **277,** 48737–48744
45. Sano, T., Baker, D. L., Virag, T., Wada, A., Yatomi, Y., Kobayashi, T., Igarashi, Y., and Tigyi, G. J. (2002) *J. Biol. Chem.* **277,** 21197–21206
46. Mulder, C., Wahlund, L. O., Teerlink, T., Blomberg, M., Veerhuis, R., van, K. G., Scheltens, P., and Scheffer, P. G. (2003) *J. Neural Transm.* **110,** 949–955
47. Pedersen, P. H., Edvardsen, K., Garcia-Cabrera, I., Mahesparan, R., Thorsen, J., Mathisen, B., Rosenblum, M. L., and Bjerkvig, R. (1995) *Int. J. Cancer* **62,** 767–771
48. Mills, G. B., Eder, A., Fang, X., Hasegawa, Y., Mao, M., Lu, Y., Tanyi, J., Tabassam, F. H., Wiener, J., Lapushin, R., Yu, S., Parrott, J. A., Compton, T., Tribley, W., Fishman, D., Stack, M. S., Gaudette, D., Jaffe, R., Furui, T., Aoki, J., and Erickson, J. R. (2002) *Cancer Treat. Res.* **107,** 259–283
49. Schulte, K. M., Beyer, A., Kohrer, K., Oberhauser, S., and Roher, H. D. (2001) *Int. J. Cancer* **92,** 249–256
50. Nam, S. W., Clair, T., Kim, Y. S., McMarlin, A., Schiffmann, E., Liotta, L. A., and Stracke, M. L. (2001) *Cancer Res.* **61,** 6938–6944
51. Bligh, E. G., and Dyer, W. J. (1959) *Can. J. BioChem. Physiol.* **37,** 911–917

THE JOURNAL OF BIOLOGICAL CHEMISTRY VOL. 281, NO. 49, pp. 37507–37516, December 8, 2006

Unique and Overlapping Transcriptional Roles of Arylhydrocarbon Receptor Nuclear Translocator (Arnt) and Arnt2 in Xenobiotic and Hypoxic Responses*

Received for publication, July 20, 2006, and in revised form, September 13, 2006 Published, JBC Papers in Press, October 5, 2006, DOI 10.1074/jbc.M606910200

Hiroki Sekine[‡], Junsei Mimura[‡§], Masayuki Yamamoto[‡], and Yoshiaki Fujii-Kuriyama[‡§1]

From the [‡]Center for Tsukuba Advanced Research Alliance and Institute of Basic Medical Sciences, University of Tsukuba, 1-1-1 Tennoudai, Tsukuba 305-8577, Japan and [§]SORST, Japan Science and Technology Agency, 4-1-8 Honcho, Kawaguchi, 332-0012 Japan

Arnt and the homologous Arnt2 share a high degree of sequence similarity and are believed to function as obligate common partners for a number of basic helix-loop-helix (bHLH)-PAS transcription factors including arylhydrocarbon receptor (AhR) and HIFα. Genetic disruption of both Arnt and Arnt2 demonstrated both unique and overlapping functions in response to environmental stimuli and during mouse development. Either stably or transiently expressed Arnt/Arnt2 wild type and various mutants or chimeric constructs in Hepa1-c4 cells exhibit similar levels of hypoxic response element-driven reporter gene expression and the induction of endogenous *Glut-1* through binding with HIFα in response to hypoxia. In contrast, we observed clear functional differences in the ability of Arnt and Arnt2 to induce xenobiotic response element-driven reporter and endogenous *CYP1A1* gene expression. In contrast with Arnt, Arnt2 was practically incapable of interacting with ligand-activated AhR to induce the expression of target genes for xenobiotic-metabolizing enzymes in response to xenobiotics. The differential binding of AhR by Arnt and Arnt2 can be ascribed to a single His/Pro amino acid difference in the PASB region of Arnt and Arnt2, suggesting that the PASB/PASB interaction between bHLH-PAS transcription factors plays a selective role for their specific partner molecule.

Arylhydrocarbon receptor nuclear translocator (Arnt)[2] is a nuclear localized transcription factor that is a canonical member of a transcription factor family consisting of an N-terminal basic helix-loop-helix (bHLH) domain followed by a PAS domain, so named because it is conserved among Per, Arnt, and Sim (1–5). In contrast, the arylhydrocarbon receptor (AhR), a member of the same transcription factor family, associates with an HSP90 complex in the cytoplasm and, upon binding an exogenous inducer such as 3-methylcholanthrene (3MC) or 2,3,7,8-tetrachlorodibenzo-*p*-dioxin (TCDD), translocates from the cytoplasm to the nucleus. Within the nucleus, AhR dissociates from HSP90 and forms a heterodimer with Arnt. The newly formed AhR·Arnt complex binds *cis*-acting DNA enhancer sequences, known as xenobiotic response element (XRE), or dioxin response element (DRE), to enhance the expression of a number of drug-metabolizing enzyme genes including cytochrome P4501A1 (*CYP1A1*) (6). Furthermore, AhR·Arnt signaling is essential for liver and palate development as well as normal reproductive homeostasis, as shown by studies on AhR-deficient mice (7, 8).

Under normoxic conditions, expression of the bHLH-PAS transcription factors hypoxia-inducible factor (HIF)-1α and HIF2α is negatively regulated by the von Hippel-Lindau tumor suppressor protein through the 26 S proteasome (9). However, under hypoxic conditions, HIFα is stabilized and translocates into the nucleus, where it forms a heterodimer with Arnt and binds the hypoxic response element (HRE) leading to the expression of target genes involved in glycolysis, erythropoiesis, and angiogenesis (6). In addition, HIF1α and HIF2α may be involved in normal embryonic development (10–12).

Arnt2, first identified as a homologue with a high degree of sequence similarity to Arnt, undergoes heterodimerization with other bHLH-PAS transcription factors, but unlike the ubiquitously expressed Arnt, Arnt2 expression is restricted to neural tissues and the kidney (13, 14). Arnt2-deficient mice die in the perinatal period and have impaired hypothalamic development (15), but targeted disruption of the Arnt gene leads to embryonic lethality between E9.5 and E10.5 characterized by disrupted placental, hematopoietic and yolk sac vascular development (16–19). When compound heterozygous $Arnt^{2+/-}$ and $Arnt^{+/-}$ mice were mated, all homozygous double mutant mice died before E8.5, and a much smaller number of compound heterozygous $Arnt^{-/-}Arnt^{2+/-}$ or $Arnt^{+/-}$ $Arnt2^{-/-}$ mutant fetuses were found to be alive at E8.5 than expected from Mendelian genetics, suggesting a strong genetic interaction between Arnt2 and Arnt during mouse development (20). Thus, although the expression and functions of Arnt2 and Arnt are not entirely overlapping, there is a strong genetic and functional interaction during development. We wished to deter-

* This work was funded in part by Solution Oriented Research for Science and Technology, Japan Science and Technology Agency and by a grant for Scientific Research from the Ministry of Health, Labor, and Welfare of Japan. The costs of publication of this article were defrayed in part by the payment of page charges. This article must therefore be hereby marked "*advertisement*" in accordance with 18 U.S.C. Section 1734 solely to indicate this fact.

[1] To whom correspondence should be addressed: Center for Tsukuba Advanced Research Alliance, University of Tsukuba, 1-1-1 Tennoudai, Tsukuba, Ibaraki 305-8577 Japan. Tel.: 81-29-853-7323; Fax: 81-29-853-7318; E-mail: ykfujii@tara.tsukuba.ac.jp.

[2] The abbreviations used are: Arnt, arylhydrocarbon receptor nuclear translocator; mArnt, mouse Arnt; 3MC, 3-methylcholanthrene; TCDD, 2,3,7,8-tetrachlorodibenzo-*p*-dioxin; bHLH, basic helix-loop-helix; AhR, arylhydrocarbon receptor; HIF, hypoxia-inducible factor; XRE, xenobiotic response element; HRE, hypoxic response element; E, embryonic day; PBS, phosphate-buffered saline; WT, wild type; aa, amino acid(s).

mine the biochemical and molecular basis for the observed differential roles of Arnt and Arnt2 in physiology and development. Although in our previous report on the transient DNA transfection experiments Arnt2 exhibited some 20% transactivation activity of Arnt with XRE-driven reporter gene (13), stably expressed Arnt2 in transformant cells failed to induce the expression of the XRE-reporter and endogenous *CYP1A1* genes in sharp contrast with studies of Arnt. Interestingly, the differential activity between Arnt and Arnt2 in heterodimer formation with AhR can be ascribed to a single amino acid replacement in the PASB domain.

EXPERIMENTAL PROCEDURES

Plasmids—mArnt and mArnt2 in pBSK were cleaved with NcoI and fused at their N termini with a 3xFLAG tag derived from p3xFLAG-CMV-10 (Sigma). pBSK3xFLAG-Arnt and pBSK3xFLAG-Anrt2 were cleaved with EcoRI and XbaI, and the isolated inserts were blunt-ended and subsequently cloned into XbaI-digested blunt-ended pEFBOS (21) to produce pBOS3xFLAG-Arnt and pBOS3xFLAG-Arnt2. Arnt/Arnt2 chimeras were produced and designated as follows: 3xFLAG-A1(A2TA); 3xFLAG-Arnt N-terminal region (aa 1–465) was connected with the Arnt2 C-terminal region (aa 440–712), 3xFLAG-A2(A1TA); 3xFLAG-Arnt2 N-terminal region (aa 1–439) was connected with the Arnt C-terminal region (aa 466–791), 3xFLAG-A1(A2AB), and 3xFLAG-A2(A1AB); 3xFLAG Arnt or Arnt2 PAS domain was replaced with the Arnt2 or Arnt PAS domain (Arnt-(156–465), Arnt2-(130–439)), respectively (see Fig. 2*A* for summary), 3xFLAG-A1(A2A); 3xFLAG-Arnt PASA domain was replaced with the Arnt2 PASA domain (Arnt-(156–356), Arnt2-(130–330)), respectively (see Fig. 5*A* for summary), 3xFLAG-A1(A2B); 3xFLAG Arnt PASB domain was replaced with the Arnt2 PASB domain (Arnt-(357–465), Arnt2-(331–439)) (see Fig. 5*A* for summary). These cDNA expression vectors were generated using the standard methods and confirmed by sequencing, and the inserts were then cloned into the pBOS vector. pBOS3xFLAG-ArntH378P, pBOS3xFLAG-A1(A2A)H378P, and pBOS-3xFLAG-A1(A2B)P352H were generated by site-directed mutagenesis using the Sculptor *in vitro* mutagenesis system (Amersham Biosciences) with pBOS3xFLAG-Arnt, pBOS3xFLAG-A1(A2A), and pBOS3xFLAG-A1(A2B), as templates, respectively (See Fig. 5*A* for summary).

For construction of pBOSGAL4DBD-Arnt-bHLHPAS-(91–465) and pBOSGAL4DBD-Arnt2-bHLHPAS-(65–439), mArnt-bHLHPAS and mArnt2-bHLHPAS region fragments were produced by PCR, using pBOS3xFLAG-Arnt and pBOS3xFLAG-Arnt2 as templates, and confirmed by sequencing. These fragments were cloned into the pBOSGAL4DBD vector (22). Chimeric constructs were produced and designated as follows: pBOSGAL4DBD-A1A2-bHLHPAS; pBOSGAL-4DBD-Arnt-bHLHPAS N-terminal region (aa 91–257) fused with the Arnt2-bHLHPAS C-terminal region (aa 232–439), pBOSGAL4DBD-A1A2A1-bHLHPAS, A1A1A2-bHLHPAS, A1A2A1–2-bHLHPAS, and A1A1A2–2-bHLHPAS. The sequences of the following regions (aa 258–333, 334–465, 334–397, and 398–465) from pBOSGAL4DBD-Arnt-bHLHPAS were exchanged, respectively, with the corresponding regions of Arnt2-(232–307), -(308–439), -(308–371), and -(372–439). pBOSGAL4DBD-ArntH378P-bHLHPAS was generated by site-directed mutagenesis using pBOSGAL4DBD-Arnt-bHLHPAS as a template.

To produce pBOSVP16AD-mHIF1αΔC, the mHIF1αΔC-(1–613) fragment was generated by PCR using cDNA from Hepa1 RNA as a template and cloned into pGEM-T-Easy vector (Promega). After sequencing, the excised cDNA fragment was inserted into pBOSVP16AD multi-cloning sites (22).

Cell Culture—Hepa1-c4 (an Arnt-defective cell line of Hepa1c1c7 cells (23)), Hepa1, 293T, and HeLa cells were maintained, respectively, in high or low glucose Dulbecco's modified Eagle's medium (Sigma) supplemented with 10% fetal bovine serum (Sigma) and penicillin/streptomycin (Invitrogen) under 5.0% CO_2 at 37 °C.

Reporter Assay—All luciferase assays were performed using the Dual-Luciferase reporter assay system according to the manufacturer's protocol (Promega) with some modifications. Hepa1-c4 cells (2.0×10^4 cells/well) were plated in 24-well plates 24 h prior to transfection. Cells were co-transfected with pXRE4-SV40-Luc (22) or pHRE6-SV40-Luc reporter (24) using 1 ng of *Renilla* luciferase as an internal control and pBOS3xFLAG-Arnt, pBOS3xFLAG-Arnt2, or the chimeric constructs using FuGENE 6 transfection reagent (Roche Applied Science) according to the manufacturer's protocol. All cells were incubated for 24 h at 37 °C after transfection. pXRE4-SV40-Luc-transfected cells were treated with 1 μM 3MC, a potent inducer of XRE-driven transcription, or with Me_2SO and then incubated for an additional 18 h. To measure hypoxia-induced transcription, cells transfected with pHRE6-SV40-Luc were incubated under normoxic or hypoxic (1.0% O_2) conditions for an additional 16 h.

HeLa cells (2.5×10^4 cells/well) were cultured in 24-well plates for 24 h prior to transfection and then were cotransfected with pXRE4-SV40-Luc or pHRE6-SV40-Luc, 1 ng of *Renilla* luciferase as an internal control, effector plasmid (pBOS3x-FLAG-Arnt, pBOS3xFLAG-Arnt2, chimeric or mutant constructs), and partner molecule plasmid (either pBOSmAhR (22) or pBOShHif1α (24)) using Lipofectamine Plus (Invitrogen) according to the manufacturer's protocol. After an additional 24 h of incubation, cells were treated with 3MC or placed under hypoxic condition as described above.

For the Arnt-AhR two-hybrid assay, 293T cells (2.0×10^4 cells/well) were cultured in 24-well plates 24 h prior to transfection and cotransfected with 100 ng of pG3-Luc (22), 0.1 ng of *Renilla* luciferase reporter as an internal control, 10 ng of the bait plasmid (either pBOSGAL4DBD-Arnt, -Arnt2-bHLHPAS, or chimeric or mutant constructs), and 60 ng of prey plasmid (either pBOSVP16AD-mAhRΔC (22) or pBOSVP16AD-mAhRΔBΔC) using Lipofectamine Plus (Invitrogen). For Arnt-HIF1α two-hybrid assay, cultured 293T cells were cotransfected with 100 ng of pG3-Luc (22), 0.1 ng of *Renilla* luciferase reporter as an internal control, 2 ng of the bait plasmid (either pBOSGAL4DBD-mArnt, pBOSGAL4DBD-mArnt2-bHLHPAS, or chimeric and mutants constructs), and 5 ng of pBOSVP16AD-mHIF1αΔC as described above. 3MC and hypoxia treatment were performed as described above.

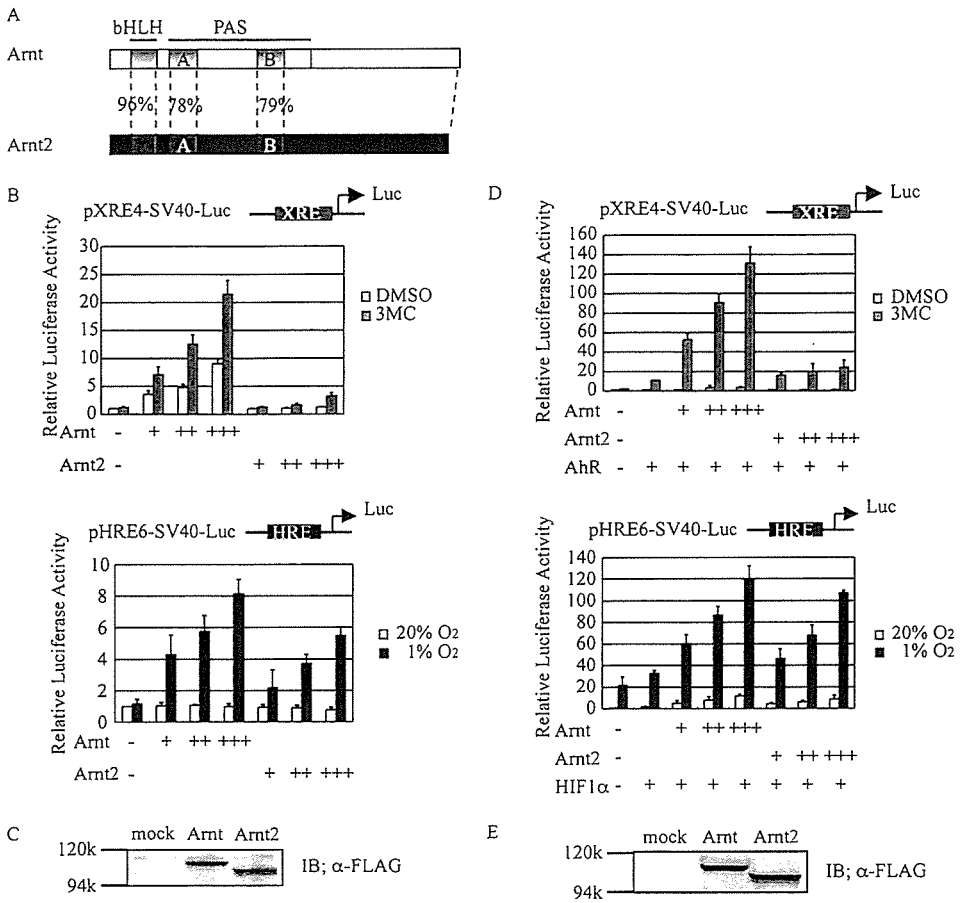

FIGURE 1. **Transcriptional activity of Arnt and Arnt2 on XRE- and HRE-driven reporter genes in Hepa1-c4 and HeLa cells.** *A*, amino acid identities between Arnt and Arnt2. *B*, transcriptional activity of Arnt and Arnt2 in Hepa1-c4 cells. Hepa1-c4 cells were transfected with 100 ng of pXRE4-SV40-Luc and increasing amounts (1, 10, and 100 ng) of 3xFLAG-Arnt or 3xFLAG-Arnt2 expression plasmids, incubated for 24 h, and treated with 1 μM 3MC or Me_2SO (dimethyl sulfoxide (*DMSO*)) for 18 h (*top panel*). For analysis of the hypoxic response, Hepa1-c4 cells were transfected with 100 ng of pHRE6-SV40-Luc and increasing amounts (1, 10, and 100 ng) of 3xFLAG-Arnt or 3xFLAG-Arnt2 expression plasmids. After 24 h of incubation, the cells were treated for 16 h under conditions of normoxia (20% O_2) or hypoxia (1% O_2) (*bottom panel*). The cell extracts were prepared from the treated cells and used for luciferase assays. Values are represented by mean ± S.D. of the results of three independent experiments normalized to *Renilla* luciferase activity used as an internal control. *C*, expression of Arnt and Arnt2 in Hepa1-c4 cells. Hepa1-c4 cells were transfected with 0.5 μg of the indicated expression construct in 6-well plates. The protein levels were evaluated by Western blotting using anti-FLAG antibody. Equal amounts of cell lysates were used for Western blot analysis. The *mock* lane represents cell lysate transfected with empty vector alone. *D*, transcriptional activity of Arnt and Arnt2 in HeLa cells. *Top panel*, XRE-driven reporter activity. HeLa cells were transfected with 10 ng of pXRE4-SV40-Luc, increasing amounts (0.1, 0.5, and 2 ng) of 3xFLAG-Arnt or -Arnt2 expression plasmids, and 10 ng of pBOSmAhR, and the reporter gene expression assays were performed as described in *B*. *Bottom panel*, HRE-driven reporter activity. HeLa cells were transfected with 10 ng of pHRE6-SV40-Luc, increasing amounts (0.1, 0.5, and 2 ng) of 3xFLAG-Arnt or -Arnt2 expression plasmids, and 20 ng of pBOShHIF1α, and the reporter gene expression assays were performed as described in *B*. Values are represented by mean ± S.D. of the results of three independent experiments normalized to *Renilla* luciferase activity used as an internal control. *E*, expression of Arnt and Arnt2 in HeLa cells. HeLa cells were transfected with 10 ng of the indicated expression construct in 6-well plates. *IB*, immunoblot.

Generation of Stable Transformant Cell Lines—Hepa1-c4 cells were cotransfected with pSVneo and effector plasmid (either pBOS3xFLAG-Arnt, pBOS3xFLAG-Arnt2, or pBOS3x-FLAG-ArntH378P). After transfection, the cells were replated and incubated with selection medium containing 0.5 mg/ml Geneticin (Invitrogen).

Western Blot Analysis—Cells were dissolved in SDS sample buffer, and proteins were separated by SDS-PAGE for Western blot analysis. Proteins were then transferred to polyvinylidene difluoride membranes and blocked in 3% skim milk for 30 min. A rabbit anti-Arnt antiserum (25) or anti-FLAG (Sigma), anti-AhR (Biomol), or anti-actin or anti-VP16AD (Santa Cruz Biotechnology) antibodies were used as primary reagents. After being washed three times in TBS (25 mM Tris/HCl (pH 7.5), 150 mM NaCl) containing 0.1% Triton X-100, membranes were incubated with species-specific horseradish peroxidase-conjugated secondary antibody (Zymed Laboratories Inc.). The protein-antibody complexes were visualized by the enhanced chemiluminescence detection system (Amersham Biosciences) according to the recommendations of the manufacturer.

Whole Cell Lysate Preparation for Coimmunoprecipitation—Hepa1-c4 cells stably transfected with pBOS-3xFLAG-Arnt, pBOS3xFLAG-Arnt2, or pBOS3xFLAG-ArntH-378P were incubated with 1 μM 3MC or Me_2SO for 2 h and washed with ice-cold phosphate-buffered saline followed by TBS. The cells were harvested by scraping, centrifuged at 5,000 rpm at 4 °C for 5 min, and suspended in TBS containing 1 mM $CaCl_2$, 1% Triton X-100, and protease inhibitor mixture (Roche Applied Science). The cells were vortexed and placed on ice for 5 min. The samples were then centrifuged at 15,000 rpm for 5 min at 4 °C, and the supernatants were reserved as whole cell lysates.

Coimmunoprecipitation Assay—The prepared whole cell lysate (200 μl) was added to 200 μl TBS with 1 mM $CaCl_2$ and protease inhibitor mixture and incubated with anti-FLAG antibody for 1 h at 4 °C. The reaction mixture was supplemented with 15 μl of protein A-agarose beads (Amersham Biosciences). After incubating for an additional 1 h at 4 °C, the beads were washed three times with TBS and resuspended in SDS sample buffer. The coimmunoprecipitated proteins were resolved by SDS-PAGE, and Western blot analysis was performed.

Immunohistochemistry—Hepa1-c4 cells stably transfected with pBOS3xFLAG-Arnt, pBOS3xFLAG-Arnt2, or pBOS3x-FLAG-ArntH378P were washed, fixed in 4% paraformaldehyde at room temperature for 10 min, and treated with cold acetone for 1 min on ice. After washing with PBS, the cells were incubated with 3% skim milk for 1 h at room temperature and treated with 10 μg/ml mouse anti-FLAG antibody for 16 h at 4 °C. After washing with PBS, the cells were subsequently

treated with biotinylated anti-mouse IgG antibody (Vector) for 3 h at 4 °C, washed with PBS, and treated with streptavidin-Alexa Fluor 488 (Invitrogen) and Hoechst solution (Dojindo) for 30 min at room temperature. After washing with PBS, a drop of fluorescent mounting medium (Dako) was placed on the cells, which were then examined by fluorescence microscopy.

Real-time PCR—Total RNA samples were prepared from the treated cells using Isogen (Nippon Gene) as described. First-strand cDNA was synthesized from 1 μg of total RNA using SuperScript reverse transcriptase (Invitrogen). Real-time PCR was performed in triplicate for each sample with the ABI Prism 7700 sequence detector (PE Applied Biosystems) using primers designed against mouse *GLUT1* (26) and *CYP1A1* (primer sequences GGTACAGAGAAAGATCCAGGAGGA and CGAA-GGATGAATGCCGGAAGGTCT and probe sequence 6-FAM-CTAGACACAGTGATTGGCAGAGATCGGCA-TAMRA) or rRNA genes (PE Applied Biosystems).

RESULTS

Comparison between Transcription Activities of Arnt and Arnt2 for Expression of the XRE- and HRE-driven Reporter Genes—It has been reported that the bHLH and PAS domains of Arnt and Arnt2 are very similar and mediate homo- and heterodimerization (Fig. 1*A*), but Arnt2 showed only 20% transcription activity of Arnt in the expression of the XRE-driven reporter gene (13).

To clarify whether the low transcription activity of Arnt2 for the expression of the XRE reporter gene is because of a low level of expression of Arnt2 or a low affinity of Arnt2 to AhR as compared with Arnt, we investigated the transcription activity of the XRE- and HRE-driven reporter genes by Arnt2 and Arnt in a dose-dependent manner using the transient transfection assay. In an experiment using either Hepa1-c4 or HeLa cells (the same result was obtained with NIH3T3 cells, data not shown), a highly inducible expression of the XRE-driven reporter gene was observed by Arnt in response to 3MC. In marked contrast, Arnt2 exhibited only a low level of inducible expression of the reporter gene even at the highest dose (Fig. 1, *B* and *D*). On the other hand, the HRE-driven reporter gene was induced similarly by Arnt and Arnt2 in response to hypoxia. Taken together with the results that Arnt and Arnt2 were similarly expressed at a protein level as shown in Fig. 1, *C* and *E*, all of these results suggest that Arnt2 is much less efficient than Arnt in conjunction with AhR for the inducible expression of the XRE reporter gene, whereas both Arnt and Arnt2 work equally well with HIFα to regulate the HRE reporter gene expression.

PAS Domain Is Responsible for Differential Activities between Arnt and Arnt2 for XRE-driven Reporter Gene Expression—We were interested in the molecular mechanisms responsible for the differences in transcriptional activity between Arnt and Arnt2. To investigate which part of the Arnt and Arnt2 molecules is responsible for the differential activity, we divided Arnt and Arnt2 into three parts based on the N-terminal bHLH, PAS, and C-terminal activation domains and generated several chimeric constructs by swapping the respective domains for Arnt and Arnt2 (Fig. 2*A*). As shown in the *upper panel* of Fig. 2*B* (*column 1 versus 3*), the luciferase activity is the same in cells

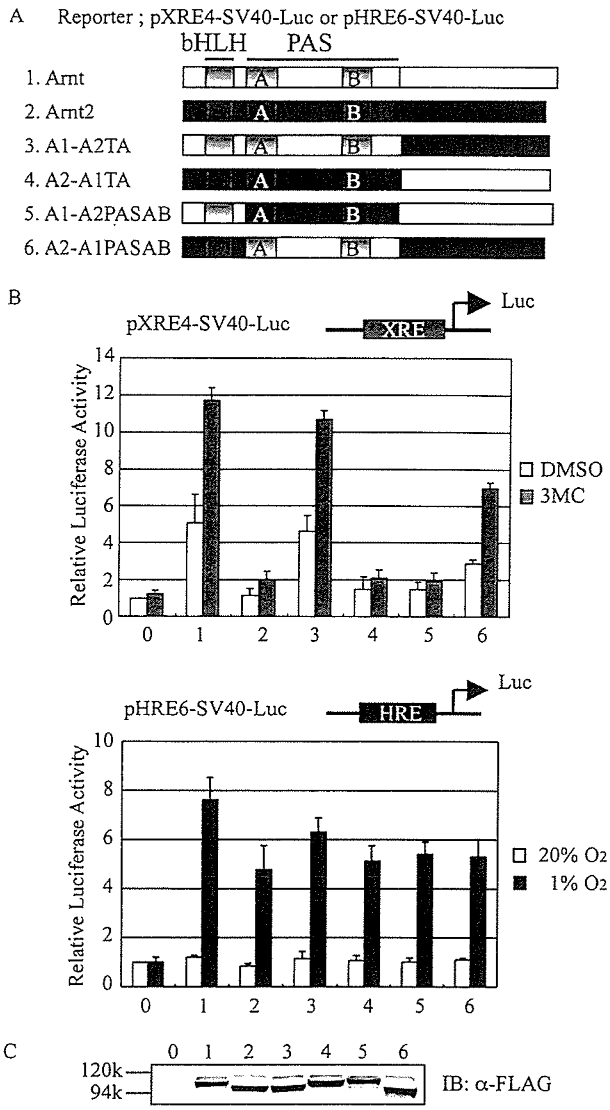

FIGURE 2. **Transcriptional activity of Arnt/Arnt2 chimeric proteins on XRE- and HRE-driven reporter genes in Hepa1-c4 cells.** *A*, Arnt and Arnt2 structures and their domain-swapping constructs. *B*, transcriptional activity of Arnt/Arnt2 chimeric constructs. Hepa1-c4 cells transfected with 100 ng of pXRE4-SV40-Luc and 10 ng of the indicated Arnt/Arnt2 chimeric constructs were incubated for 24 h and then treated with 1 μM 3MC or Me_2SO (dimethyl sulfoxide (*DMSO*)) for 18 h (*top panel*). For analysis of the hypoxic response, Hepa1-c4 cells were transfected with 100 ng of pHRE6-SV40-Luc and 10 ng of the Arnt/Arnt2 chimeric constructs. After 2 h of incubation, the cells were treated for 16 h under normoxia or hypoxia (1% O_2) (*bottom panel*). The cell extracts were prepared from the treated cells and used for luciferase assays. Values are represented by mean ± S.D. of the results of three independent experiments normalized to *Renilla* luciferase activity used as an internal control. *C*, expression of Arnt, Arnt2, and chimeric constructs. The cells were transfected with 50 ng of the indicated expression construct in 6-well plates. The protein levels of all constructs were evaluated by Western blotting using anti-FLAG antibody. Equal amounts of cell lysates were used for Western blot analysis. *Columns* in *B* and *C*: *0*, pBOS; *1*, pBOS3xFLAG-Arnt; *2*, pBOS3xFLAG-Arnt2; *3*, pBOS3xFLAG-A1(A2TA); *4*, pBOS3xFLAG-A2(A1TA); *5*, pBOS3xFLAG-A1(A2AB); *6*, pBOS3xFLAG-A2(A1AB). *IB*, immunoblot.

expressing WT Arnt and a chimera composed of the N-terminal bHLH and PAS domains of Arnt and the C-terminal region of Arnt2. In contrast, a chimera composed of the bHLH and C-terminal domains of Arnt and the PAS domain of Arnt2 activates only a low level of luciferase expression, as observed with WT Arnt2 for the expression of XRE-driven reporter gene (Fig.

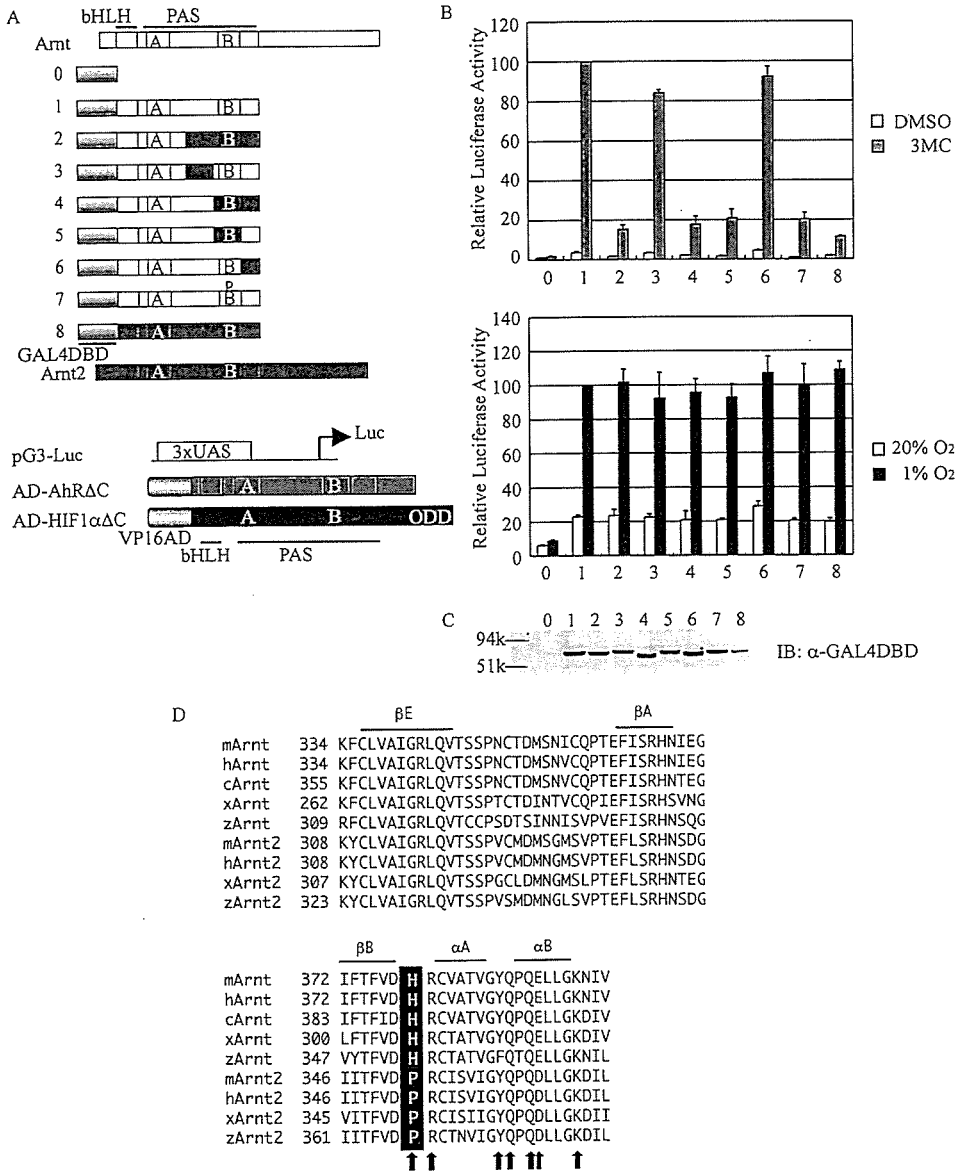

FIGURE 3. **Two-hybrid analysis of transcriptional activities of Arnt and Arnt2 and their chimeric and mutant derivatives.** *A*, constructs of bait proteins of Arnt and Arnt2, their chimeras and mutant, and prey molecules of AhR and HIF1α. *B*, transcriptional activity of various Arnt/Arnt2-bHLHPAS chimeric proteins in the two-hybrid system. 293T cells were transfected with pG3-Luc, the indicated Arnt/Arnt2 construct, and pBOSVP16AD-mAhRΔC (*AD-AhRΔC*) or pBOSVP16AD-mHIF1αΔC (*AD-HIF1αΔC*) (see "Experimental Procedures"). The transfected cells were treated as described in the legend to Fig. 1*B*. *Top panel*, relative luciferase activities induced by 3MC treatment. *Bottom panel*, relative luciferase activities induced by hypoxic treatment. Values are represented by mean ± S.D. of the results of three independent experiments normalized to *Renilla* luciferase activity used as internal control. *DMSO*, dimethyl sulfoxide (Me_2SO). *C*, expression of the bait proteins. The cells were transfected with 50 ng of the indicated expression construct in 6-well plates. Protein levels of all constructs were evaluated by Western blot analysis using α-GAL4DBD antibody. The cells were homogenized, and supernatants were subjected to SDS-PAGE for Western blot analysis (*IB*, immunoblot). *Columns*: *0*, pBOSGAL4DBD; *1*, pBOSGAL4DBD-Arnt-bHLHPAS; *2*, pBOSGAL4DBD-Arnt2-bHLHPAS; *3*, pBOSGAL4DBD-A1A2-bHLHPAS; *4*, pBOSGAL4DBD-A1A2A1–1-bHLHPAS; *5*, pBOSGAL4DBD-A1A1A2–1-bHLHPAS; *6*, pBOSGAL4DBD-A1A2A1–2-bHLHPAS; *7*, pBOSGAL4DBD-A1A1A2–2-bHLHPAS; *8*, pBOSGAL4DBD-ArntH378P-bHLHPAS (see "Experimental Procedures"). The full activity of *column 1* was taken as a standard to calculate relative activities. *D*, amino acid sequences of a part of PASB region of Arnt and Arnt2 responsible for differential transcriptional activities in association with AhR. Predicted exposed side chains of amino acids (27) are indicated by *arrows*. *m*, mouse; *h*, human; *c*, chicken; *x*, *Xenopus*; *z*, zebrafish.

2*B*, *upper panel*, *columns 2* and *5*). Thus, it is not the highly variable C-terminal domain but the PAS domain that is responsible for the differences in XRE-driven luciferase expression. In contrast, any combination of Arnt and Arnt2 domains was able to activate luciferase expression to the same extent in response to hypoxia. Taken together, these results suggest that only the PAS domain of Arnt is capable of efficient heterodimerization with AhR to activate the XRE, but HIFα interacted equally with the PAS domains of Arnt and Arnt2 leading to HRE-mediated transcription.

Interaction of the PAS Domains of Arnt or Arnt2 with Those of AhR and HIF1α—To further investigate the interaction of the PAS domains of Arnt and Arnt2 with AhR, we used a mammalian two-hybrid system. Arnt/Arnt2 bHLH-PAS chimeric constructs fused with the GAL4DBD were used as bait, and AhRΔC or HIF1αΔC fused with the VP16 activation domain were used as preys (Fig. 3*A*). Replacement of only a small portion of the PASB domain of Arnt with that of Arnt2 almost completely abrogated 3MC-induced luciferase expression (Fig. 3*B*, *upper panel*, *columns 2*, *4*, and *5 versus 1*, *3*, and *6*). All constructs were equally expressed except for a slightly lower expression of construction 8 (Fig. 3*C*). Taken together, these data indicate that the critical region for determining the differential interaction of Arnt and Arnt2 with AhR covers the sequence of amino acids 334–397 of Arnt and 308–371 of Arnt2. This region is predicted to form the N-terminal cap and a part of the PAS core of the PASB fold and is thought to be solvent-exposed, forming an interface to interact with partner proteins (27). In this region there are seven amino acids with side chains that are predicted to be solvent-exposed (27) (indicated by *arrows* in Fig. 3*D*), and six are conserved or conservative amino acid replacements between Arnt and Arnt2. Only the replacement of His with Pro was considered to be significant for the functional difference between Arnt and Arnt2. These amino acids, His and Pro, are conserved, respectively, in Arnt and Arnt2 of various animal species (Fig. 3*D*). When we generated a His-to-Pro point mutation in Arnt, this construct was not able to interact efficiently with AhR to activate luciferase expression in response to 3MC (Fig. 3*B*, *upper panel*, *column 7*). On the other hand, all chimeric constructs, WT Arnt and Arnt2, and

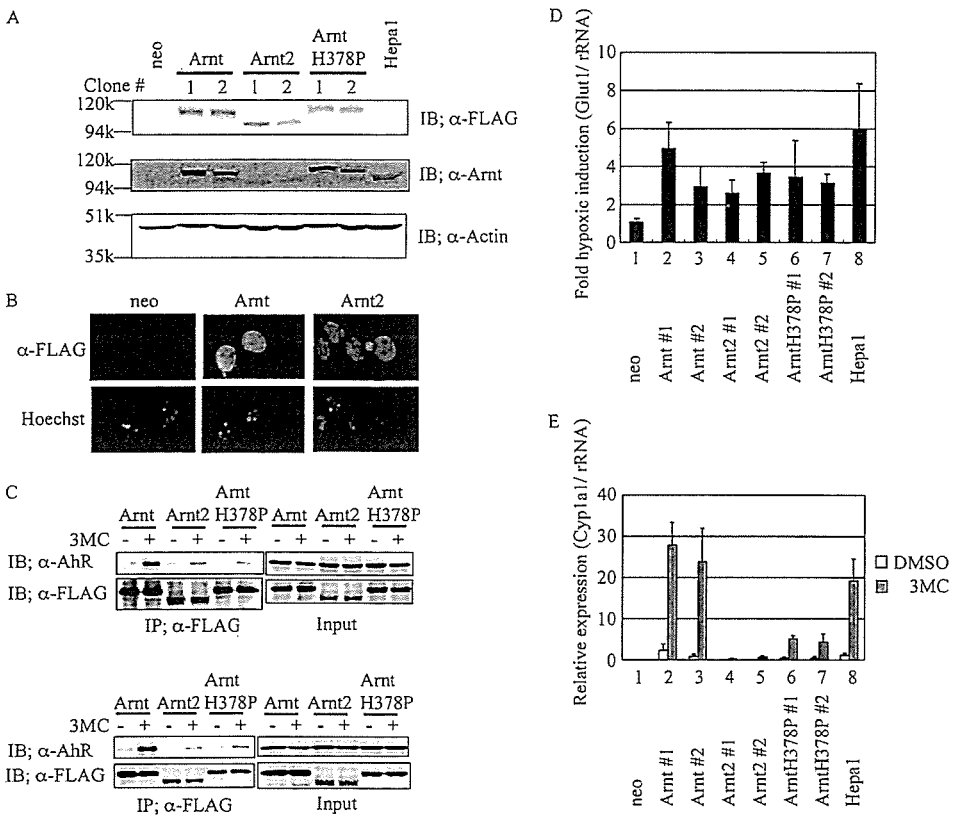

FIGURE 4. **Transcriptional activities of Arnt, Arnt2 and ArntH378P mutant in stably transformed Hepa1-c4 cells.** *A*, expression of 3xFLAG-Arnt, -Arnt2, and -ArntH378P. Expressed proteins were assessed by Western blotting (*IB*, immunoblot) using anti-Arnt, anti-FLAG, and anti-actin antibodies. *B*, cellular localization of 3xFLAG-Arnt and 3xFLAG-Arnt2. Hepa1-c4 cells stably expressing 3xFLAG-Arnt and 3xFLAG-Arnt2 were fixed and immunostained for Arnt and Arnt2 with anti-FLAG antibody. *C*, coimmunoprecipitation of AhR with Arnt, Arnt2, and ArntH378P in response to 3MC. Whole cell extracts of transformants expressing 3xFLAG-Arnt, 3xFLAG-Arnt2, and 3xFLAG-ArntH378P treated with 3MC or Me_2SO (dimethyl sulfoxide (*DMSO*)) were coimmunoprecipitated by anti-FLAG antibody. Coimmunoprecipitation and Western blotting were performed by the methods described under "Experimental Procedures." The *top* and *bottom left panels* show AhR and 3xFLAG-Arnts proteins coimmunoprecipitated by anti-FLAG antibody. *Input* is shown in the *right panels*. The *upper* and *lower panels* represent clone 1 and clone 2, respectively. *D*, expression of endogenous *Glut-1* gene in transformants expressing 3xFLAG-Arnt, -Arnt2, and -ArntH378. Transformed Hepa1-c4 cells were cultured for 16 h under conditions of normoxia or hypoxia (1% O_2), and cell extracts were prepared and used for determination of Glut-1 mRNA expression by real-time PCR analysis. Values are normalized against those for rRNA, and the results are expressed as induction ratios of hypoxic to normoxic activities. *E*, Expression of endogenous *CYP1A1* gene in the transformants. Stably transformed Hepa1-c4 cells were treated with Me_2SO or 3MC for 18 h, and the cell extracts were prepared and used for determination of CYP1A1 mRNA by real-time PCR analysis.

the Arnt His-to-Pro mutant induced luciferase expression to the same extent in response to hypoxia (Fig. 3*B*, *lower panel*). These data indicate that a single amino acid change is mainly responsible for the differential binding of Arnt and Arnt2 with AhR, whereas both Arnt and Arnt2 are equally capable of binding with HIFα.

Physical Interaction and Transcriptional Activity of Arnt and Arnt2 with AhR in Stable Transformants—Up to this point, we have studied the activity and interactions of WT Arnt and Arnt2 and their mutants with AhR and HIFα using relatively artificial transient transfection and two-hybrid assays. We wanted to examine the behavior of these proteins in a more physiologic setting, and we generated Hepa1-c4 cells stably expressing 3xFLAG-Arnt, -Arnt2, and -ArntH378P as described under "Experimental Procedures."

For each construct we isolated two clones with 3xFLAG-Arnt/Arnt2 expression levels comparable with endogenous Arnt in unmodified Hepa1 cells (Fig. 4*A*) and the stably expressed 3xFLAG-Arnt, -Arnt2, and -ArntH378P (data not shown) proteins localized to the nucleus (Fig. 4*B*) (28). To evaluate the interaction between endogenous AhR and these stably expressed 3xFLAG-Arnt, -Arnt2, and -ArntH378P proteins, AhR-3xFLAG-Arnt coimmunoprecipitation assays were performed. In the absence of cellular treatment with 3MC, AhR was not coimmunoprecipitated with 3xFLAG-tagged Arnt, Arnt2, or ArntH378P by an anti-FLAG antibody. However, following incubation of cells with 3MC, AhR was coimmunoprecipitated with 3xFLAG-Arnt by using anti-FLAG antibody, but only a small amount of AhR was detected in the anti-FLAG immunoprecipitates from two transformant cell lines expressing 3xFLAG-Arnt2 or 3xFLAG-ArntH378P (Fig. 4*C*). These results are consistent with the reduced affinity of Arnt2 or the ArntH378P mutant for AhR as revealed in the mammalian two-hybrid system (Fig. 3*B*, *top panel*, *columns 1*, *7*, and *8*), but they are at odds with a previous study from our laboratory (13). In that report, we incubated *in vitro* translated Arnt and Arnt2 with AhR produced in Sf2 cells. It is likely that the relatively high concentrations of Arnt2 and AhR produced in the *in vitro* incubation system gave rise to a misleadingly significant band.

We next investigated the transcriptional activity of Arnt, Arnt2, and the ArntH378P mutant in the generated stable transformant cells, and we chose to examine Glut-1 and CYP1A1 induction by quantitative real-time PCR as target genes for HIF1α and AhR, respectively (29, 30). In cells expressing 3xFLAG-Arnt, -Arnt2, or -ArntH378P, Glut-1 was induced to a similar extent under hypoxic conditions when mRNA levels were normalized to normoxic cells (Fig. 4*D*). In contrast, treatment of cells stably expressing 3xFLAG-Arnt with 3MC dramatically increased CYP1A1 mRNA levels compared with untreated cells, and little induction was seen in cells expressing 3xFLAG-Arnt2 (Fig. 4*E*). Cells expressing 3xFLAG-ArntH378P slightly, but significantly, increased CYP1A1 mRNA levels following 3MC treatment, indicating that His-378 in the Arnt PASB domain strongly influences Arnt binding to AhR but that other regions of Arnt also contribute to AhR binding.

The Arnt PASA and PASB Domains Cooperatively Bind AhR—We saw some degree of *CYP1A1* transcription in response to 3MC in cells expressing 3xFLAG-ArntH378P, and we were

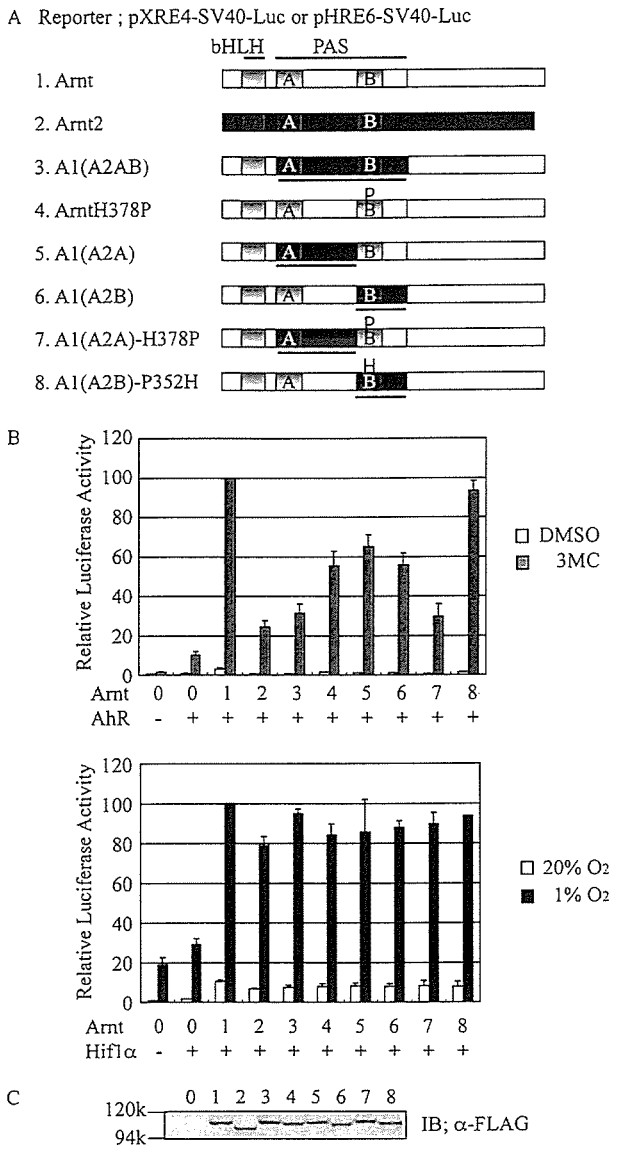

FIGURE 5. **Contribution of PASA and PASB sequences of full-length Arnt and Arnt2 to the expression of XRE-driven and HRE-driven reporter genes.** *A*, constructs of the expression plasmids of Arnt and Arnt2 and their chimeric and mutant proteins. *Underlines* show the Arnt domain replaced by the corresponding Arnt2 domain (*constructs 3* and *5–8*). *B, top*, expression of the XRE-driven reporter gene. HeLa cells were transfected with 10 ng of pXRE4-SV40-Luc, 2 ng of the indicated expression plasmid, and 20 ng of pBOSmAhR, and the reporter gene expression assay was performed as described in the legend to Fig. 1*B*. *DMSO*, dimethyl sulfoxide (Me_2SO). *Bottom*, expression of the HRE-driven reporter gene. HeLa cells were transfected with 10 ng of pHRE6-SV40-Luc, 2 ng of the indicated expression plasmid, and 20 ng of pBOShHIF1α, and the reporter gene expression assay was performed as described in the legend to Fig. 1*B*. Values are represented by mean ± S.D. of the results of three independent experiments normalized to *Renilla* luciferase activity used as an internal control. The full activity of *column 1* was taken as a standard to calculate relative activities. *C*, concentrations of the expressed effector proteins. The cells were transfected with 10 ng of the indicated expression construct in 6-well plates. Equal amounts of cell lysates were used for determination of the expressed proteins. *Columns* in *B* and *C*: *0*, pBOS; *1*, pBOS3xFLAG-Arnt; *2*, pBOS3xFLAG-Arnt2; *3*, pBOS3xFLAG-A1(A2AB); *4*, pBOS3xFLAG-ArntH378P; *5*, pBOS3x-FLAG-A1(A2A); *6*, pBOS3xFLAG-A1(A2B); *7*, pBOS3xFLAG-A1(A2A)H378P; *8*, pBOS3xFLAG-A1(A2B)P352H. *IB*, immunoblot.

interested in determining other regions of Arnt that support its interaction with AhR. Toward this end, we generated several additional Arnt/Arnt2 chimeric constructs (Fig. 5*A*) and investigated their ability to interact with AhR by luciferase reporter assay. As shown above, all WT and chimeric Arnt and Arnt2 constructs were able to induce luciferase expression in response to hypoxia when coexpressed with HIF1α (Fig. 5*B*, *lower panel*). As expected, Arnt induced XRE-driven luciferase expression to a greater extent than Arnt2, but some luciferase expression was seen in Arnt2-expressing cells compared with untreated cells as reported in our previous study (13) (Fig. 5*B*, *upper panel*, *columns 0*, *1*, and *2*). The physiologic significance of this induction is questionable, however, given the inability of stably expressed Arnt2 to induce the expression of the endogenous *CYP1A1* gene (Fig. 4*E*, *columns 4* and *5*); the ability of Arnt2 to induce luciferase in response to 3MC may be an overexpression artifact. Substitution of the Arnt PASA and PASB domains with those of Arnt2 led to reduced luciferase expression comparable with WT Arnt2 (Fig. 5*B*, *upper panel*, *columns 2*, and *3*). Additionally, the H378P mutation as well as swapping the PASA or PASB domain of Arnt2 led to intermediate levels of luciferase expression (Fig. 5*B*, *upper panel*, *columns 4*, *5*, and *6*), indicating that the PASA domain is largely responsible for the additional AhR binding activity of Arnt. Interestingly, replacement of the Arnt PASA domain with that of Arnt2 and mutation of His-378 to Pro led to luciferase expression comparable with that of WT Arnt2 (column 7), thus confirming the importance of the two regions for Arnt·AhR binding. In contrast, when the Pro residue of the Arnt2 PASB domain was mutated to His, and this mutant PASB domain replaced the corresponding one in Arnt, luciferase expression in response to 3MC was restored to WT Arnt levels (Fig. 5*B*, *upper panel*, *column 8*). As expected from the two-hybrid assay, all WT and chimeric Arnt/Arnt2 constructs behaved similarly in response to hypoxia (Fig. 5*B*, *lower panel*).

The PASB Domain of AhR Is Responsible for Differential Binding to Arnt and Arnt2—A single amino acid change largely impaired the ability of Arnt to bind AhR, and we determined the region of AhR that interacts with Arnt PASB. We used a mammalian two-hybrid system with GAL4DBD-fused Arnt, Arnt2, and the Arnt mutant as bait (Fig. 3*A*, *constructs 1*, *7*, and *8*). When we used VP16AD-AhRΔC (Fig. 6*A*) as prey together with GAL4DBD-Arnt-bHLHPAS, the reporter gene was strongly induced following 3MC treatment (Fig. 6*B*, *column 4*). Expression of a VP16AD-AhRΔBΔC construct (Fig. 6*A*) further lacking the AhR PASB region constitutively expressed a high degree of luciferase activity, although a slight inducibility remained with 3MC (Fig. 6*B*, *column 5*). The PASB region of AhR binds the HSP90 complex, and in its absence, AhR is not retained in the cytoplasm and mediates transcription in the absence of stimuli (31–33). In contrast, in cells expressing both GAL4DBD-Arnt2-bHLHPAS and VP16AD-AhRΔC, reporter gene expression was reduced remarkably and was only slightly inducible (Fig. 6*B*, *column 10*). In stark contrast, coexpression of the PASB-deleted construct VP16AD-AhRΔBΔC with GAL4DBD-Arnt2-bHLHPAS led to constitutive luciferase activity comparable with that seen with GAL4DBD-Arnt-bHLHPAS (Fig. 6*B*, *column 5 versus 11*). These results indicate that the bHLH and PASA domains of AhR are able to interact with Arnt and Arnt2 to an equal extent to mediate constitutive transcriptional activity. Addition of the PASB region of AhR, how-

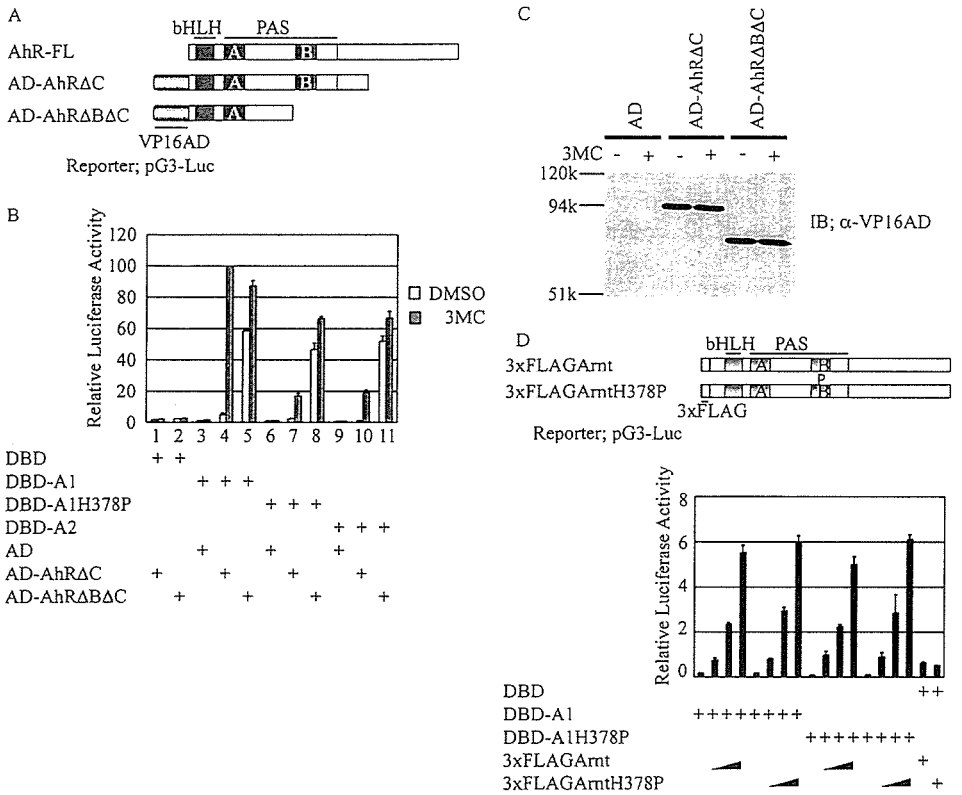

FIGURE 6. **PASB/PASB interaction is important for specific AhR/Arnt heterodimerization.** *A*, constructs of VP16AD-AhRΔC (*AD-AhRΔC*) and VP16AD-AhRΔBΔC (*AD-AhRΔBΔC*) used as prey. *B*, reporter gene expression. 293T cells were transfected with pG3-Luc, the indicated bait plasmid (pBOSGAL4DBD (*DBD*), pBOSGAL4DBD-Arnt-bHLHPAS (*DBD-A1*), pBOSGAL4DBD-ArntH378P-bHLHPAS (*DBD-A1H378P*), or pBOSGAL4DBD-Arnt2-bHLHPAS (*DBD-A2*)), and the indicated prey plasmid (pBOSVP16AD (*AD*), pBOSVP16AD-mAhRΔC, or pBOSVP16AD-mAhRΔBΔC), and after 24 h of incubation, the cells were treated with 1 μM 3MC or Me_2SO (dimethyl sulfoxide (*DMSO*)) for 18 h. Values are represented by mean ± S.D. of the results of three independent experiments normalized to *Renilla* luciferase activity used as an internal control. The full activity of *column 1* was taken as a standard to calculate relative activities. *C*, protein expression. The cells were transfected with 50 ng of the indicated expression construct in 6-well plates. The protein levels of all constructs were evaluated by Western blotting (*IB*, immunoblot) using anti-VP16AD antibody. Equal amounts of cell lysates were used for gel electrophoresis. *Columns 1* and *2*, pBOSVP16AD (*AD*); *columns 3* and *4*, pBOSVP16AD-mAhRΔC (*AD-AhRΔC*); *columns 5* and *6*, pBOSVP16AD-mAhRΔBΔC (*AD-AhRΔBΔC*). In *columns 1*, *3*, and *5*, cells were treated with Me_2SO for 18 h; in *columns 2*, *4*, and *6*, cells were treated with 1 μM 3MC for 18 h. *D*, effect of H378P mutation on Arnt/Arnt homodimerization. *Top*, 3xFLAG-Arnt and 3xFLAG-ArntH378P were used as activators. *Bottom*, expressed luciferase activities from Arnt/Arnt interaction. 293T cells were transfected with 100 ng of pG3-Luc and 10 ng of the indicated bait vectors (pBOSGAL4DBD, pBOSGAL4DBD-Arnt-bHLHPAS, or pBOSGAL4DBD-ArntH378P-bHLHPAS) and the indicated prey vector (50 ng of pBOS or 10, 20, or 50 ng of pBOS3xFLAG-Arnt or pBOS3xFLAG-ArntH378P). After 24 h of culture, the medium was changed, and the cells were further cultured for 24 h. The cell extracts were prepared from the cultured cells and used for luciferase assays. Values are represented by mean ± S.D. of the results of three independent experiments normalized to *Renilla* luciferase activity used as an internal control.

ever, specifically inhibited its interaction with Arnt2, leading to reduced reporter gene expression. Thus, the PASB domain of AhR determines its binding specificity for Arnt.

We next examined the ability of the His-378 to Pro Arnt mutant to interact with AhR; it behaved virtually identically to Arnt2 (Fig. 6*B*, *columns 7* and *8 versus 10* and *11*), indicating that Pro-352 in Arnt2 is primarily responsible for its reduced affinity for AhR. In these experiments, the prey proteins were expressed almost equally (Fig. 6*C*).

Homodimerization of Arnt and Arnt H378P—Arnt can form a heterodimer with AhR and HIF1α, but it also homodimerizes and binds E-box sequences (25, 34, 35). We investigated the ability of ArntH378P to homodimerize with either WT or mutant Arnt, using the mammalian two-hybrid assay with GAL4DBD-Arnt-bHLHPAS or GAL4DBD-ArntH378P-bHLHPAS as bait (Fig. 3*A*, *constructs 1* and *7*) and a full-length 3xFLAG-Arnt or its H378P mutant as prey (Fig. 5*A*, *constructs 1* and *4*). In any combination of bait and prey, both WT and H378P mutant Arnt activated similar levels of reporter gene expression (Fig. 6*D*), indicating that Arnt homodimerization is not sensitive to the H378P mutation. This result also suggests that Arnt PASB His-to-Pro mutation influences specifically AhR-Arnt dimerization, not the general dimerization.

DISCUSSION

Arnt and Arnt2 are structurally very similar and are believed to be common obligate dimerization partners for a number of bHLH-PAS transcription factors including AhR, HIFα, and Sims (13). We found no differences in the ability of Arnt, Arnt2, or any mutant or chimeric constructs used to activate gene expression in response to hypoxia in both transient and stable expression systems, suggesting that both proteins are equally able to bind HIFα, the key transcription factor mediating the hypoxic response. Thus, Arnt and Arnt2 play functionally interchangeable and overlapping roles in glycolysis, erythropoiesis, and angiogenesis in response to hypoxic conditions. The compensatory effects of Arnt and Arnt2 are noticeable in central nervous system development where Arnt2 is expressed abundantly (36, 37). Whole-mount PECAM (platelet endothelial cell adhesion molecule) immunohistochemistry on the embryonic central nervous system revealed no obvious differences between the WT and $Arnt2^{-/-}$ embryos, whereas $Arnt^{-/-}$ embryos had clear disruptions of the vascular endothelial network (20). This observation suggests that the expression of *VEGF* and other HIFα target genes in $Arnt2^{-/-}$ embryos is effectively normal, presumably because of the compensatory effects of Arnt. In the later stage of central nervous system development, however, several unique functions of Arnt2 become apparent, and $Arnt2^{-/-}$ embryos die perinatally with impaired hypothalamic development (15).

In contrast to their overlapping ability to bind HIFα, and also in apparent contrast with a previous report (13), clear differences were seen in the ability of Arnt and Arnt2 to interact with AhR. XRE-driven luciferase activity in cells expressing Arnt2 was much less than that seen in cells expressing Arnt following

3MC treatment, and the transcription of an XRE-responsive endogenous gene, *CYP1A1*, was completely absent in Hepa1-c4 cells stably expressing Arnt2 after treatment with 3MC (Fig. 4*E*, *columns 4* and *5*). In contrast, Hepa1-c4 cells stably expressing Arnt induced high levels of *CYP1A1* transcripts following 3MC treatment (Fig. 4*E*, columns 2 and 3). Some activation of the XRE-driven reporter gene by Arnt2 (about one-fifth of the Arnt activation) in the previous report (13) is misleading, most probably because of overexpression of Arnt2 in the transient DNA transfection experiments. Arnt2 expressed in these transformant cells was clearly functional, as shown by its ability to induce HRE-responsive genes in conjunction with HIFα (Fig. 4*D*), suggesting that Arnt2 plays little or no role in the cellular response to xenobiotics to induce the XRE-inducible genes in conjunction with AhR. This conclusion is further supported by the observation that zebrafish injected with a zfArnt2 antisense morpholino induced zfCYP1A1 in response to TCDD- as well as sham-treated animals, and there were no differences in TCDD-induced cytotoxicities requiring Arnt/AhR dimerization, such as pericardial edema, reduced trunk blood flow, and shortened lower jaw between these animals (38).

The bHLH domain of AhR is thought to be essential for heterodimer formation between bHLH-PAS transcription factors, and the bHLH domain alone of AhR is capable of dimerizing with the unrelated bHLH-Zip transcription factor USF (39). When the PASA domain is added to the AhR bHLH domain, however, AhR becomes much less promiscuous and stably binds Arnt (39). We showed that a construct consisting of the AhR bHLH and PASA domains binds both Arnt and Arnt2 (Fig. 6*B*, *columns 5* and *11*), but the addition of the PASB domain restricts AhR binding exclusively to Arnt (Fig. 6*B*, *columns 4* and *10*). Taken together, these data indicate that Arnt2 is not likely involved in the induction of drug-metabolizing enzymes following exposure to exogenous aromatic chemicals and other biological processes requiring AhR as a transcription factor.

A recent study reported that both the PASA and PASB domains of HIFα are necessary for heterodimer formation with Arnt (40). The minimal PAS domain structure consists of a 3-stranded β sheet, designated the β-scaffold, and a central α-helical PAS core region containing three short stretches of α-helices and β-sheets connected by a single α-helix called the helical connector. Mutational analysis revealed that hydrophobic interactions between conserved amino acids on the surface of the β-scaffold of HIFα and Arnt are important for heterodimerization, and replacement of hydrophilic amino acids (Q322E, M338E, and Y342T in HIF2α) disrupted this interaction leading to reduced transcription activity in response to hypoxia (40–42). Replacement of His-378 with Pro in Arnt, a residue a little away from the β-scaffold, disrupted its interaction with AhR but had no effect on the interaction of Arnt with HIFα. This suggests that the PASB/PASB-interacting surfaces or modes of AhR and Arnt are different from those of HIFα and Arnt. Additionally, the structural basis for the inhibition of AhR binding by Pro-352 of Arnt2, without affecting HIFα binding, should be examined. Such studies could provide valuable insight into the molecular regulation of the xenobiotic response as well as the diversification of a highly conserved family of transcription factors.

Acknowledgments—We thank Dr. O. Hankinson for kindly providing Hepa1-c4 mutant and Y. Nemoto for clerical work.

REFERENCES

1. Jackson, F. R., Bargiello, T. A., Yun, S. H., and Young, M. W. (1986) *Nature* **320,** 185–188
2. Reddy, P., Jacquier, A. C., Abovich, N., Petersen, G., and Rosbash, M. (1986) *Cell* **46,** 53–61
3. Hoffman, E. C., Reyes, H., Chu, F. F., Sander, F., Conley, L. H., Brooks, B. A., and Hankinson, O. (1991) *Science* **252,** 954–958
4. Crews, S. T., Thomas, J. B., and Goodman, C. S. (1988) *Cell* **52,** 143–151
5. Nambu, J. R., Lewis, J. O., Wharton, K. A., Jr., and Crews, S. T. (1991) *Cell* **67,** 1157–1167
6. Kewley, R. J., Whitelaw, M. L., and Chapman-Smith, A. (2004) *Int. J. Biochem. Cell Biol.* **36,** 189–204
7. Schmidt, J. V., Su, G. H., Reddy, J. K., Simon, M. C., and Bradfield, C. A. (1996) *Proc. Natl. Acad. Sci. U. S. A.* **93,** 6731–6736
8. Baba, T., Mimura, J., Nakamura, N., Harada, N., Yamamoto, M., Morohashi, K., and Fujii-Kuriyama, Y. (2005) *Mol. Cell. Biol.* **25,** 10040–10051
9. Huang, L. E., Gu, J., Schau, M., and Bunn, H. F. (1998) *Proc. Natl. Acad. Sci. U. S. A.* **95,** 7987–7992
10. Ryan, H. E., Lo, J., and Johnson, R. S. (1998) *EMBO J.* **17,** 3005–3015
11. Iyer, N. V., Kotch, L. E., Agani, F., Leung, S. W., Laughner, E., Wenger, R. H., Gassmann, M., Gearhart, J. D., Lawler, A. M., Yu, A. Y., and Semenza, G. L. (1998) *Genes Dev.* **12,** 149–162
12. Tian, H., Hammer, R. E., Matsumoto, A. M., Russell, D. W., and McKnight, S. L. (1998) *Genes Dev.* **12,** 3320–3324
13. Hirose, K., Morita, M., Ema, M., Mimura, J., Hamada, H., Fujii, H., Saijo, Y., Gotoh, O., Sogawa, K., and Fujii-Kuriyama, Y. (1996) *Mol. Cell. Biol.* **16,** 1706–1713
14. Drutel, G., Kathmann, M., Heron, A., Schwartz, J. C., and Arrang, J. M. (1996) *Biochem. Biophys. Res. Commun.* **225,** 333–339
15. Hosoya, T., Oda, Y., Takahashi, S., Morita, M., Kawauchi, S., Ema, M., Yamamoto, M., and Fujii-Kuriyama, Y. (2001) *Genes Cells* **6,** 361–374
16. Maltepe, E., Schmidt, J. V., Baunoch, D., Bradfield, C. A., and Simon, M. C. (1997) *Nature* **386,** 403–407
17. Kozak, K. R., Abbott, B., and Hankinson, O. (1997) *Dev. Biol.* **191,** 297–305
18. Adelman, D. M., Gertsenstein, M., Nagy, A., Simon, M. C., and Maltepe, E. (2000) *Genes Dev.* **14,** 3191–3203
19. Abbott, B. D., and Buckalew, A. R. (2000) *Dev. Dyn.* **219,** 526–538
20. Keith, B., Adelman, D. M., and Simon, M. C. (2001) *Proc. Natl. Acad. Sci. U. S. A.* **98,** 6692–6697
21. Mizushima, S., and Nagata, S. (1990) *Nucleic Acids Res.* **18,** 5322
22. Mimura, J., Ema, M., Sogawa, K., and Fujii-Kuriyama, Y. (1999) *Genes Dev.* **13,** 20–25
23. Numayama-Tsuruta, K., Kobayashi, A., Sogawa, K., and Fujii-Kuriyama, Y. (1997) *Eur. J. Biochem.* **246,** 486–495
24. Ema, M., Taya, S., Yokotani, N., Sogawa, K., Matsuda, Y., and Fujii-Kuriyama, Y. (1997) *Proc. Natl. Acad. Sci. U. S. A.* **94,** 4273–4278
25. Sogawa, K., Nakano, R., Kobayashi, A., Kikuchi, Y., Ohe, N., Matsushita, N., and Fujii-Kuriyama, Y. (1995) *Proc. Natl. Acad. Sci. U. S. A.* **92,** 1936–1940
26. Park, S. K., Dadak, A. M., Haase, V. H., Fontana, L., Giaccia, A. J., and Johnson, R. S. (2003) *Mol. Cell. Biol.* **23,** 4959–4971
27. Pellequer, J. L., Wager-Smith, K. A., Kay, S. A., and Getzoff, E. D. (1998) *Proc. Natl. Acad. Sci. U. S. A.* **95,** 5884–5890
28. Eguchi, H., Ikuta, T., Tachibana, T., Yoneda, Y., and Kawajiri, K. (1997) *J. Biol. Chem.* **272,** 17640–17647
29. Wood, S. M., Gleadle, J. M., Pugh, C. W., Hankinson, O., and Ratcliffe, P. J. (1996) *J. Biol. Chem.* **271,** 15117–15123
30. Ko, H. P., Okino, S. T., Ma, Q., and Whitlock, J. P., Jr. (1996) *Mol. Cell. Biol.* **16,** 430–436
31. Coumailleau, P., Poellinger, L., Gustafsson, J. A., and Whitelaw, M. L. (1995) *J. Biol. Chem.* **270,** 25291–25300
32. Whitelaw, M. L., Gottlicher, M., Gustafsson, J. A., and Poellinger, L. (1993) *EMBO J.* **12,** 4169–4179

33. McGuire, J., Okamoto, K., Whitelaw, M. L., Tanaka, H., and Poellinger, L. (2001) *J. Biol. Chem.* **276,** 41841–41849
34. Antonsson, C., Arulampalam, V., Whitelaw, M. L., Pettersson, S., and Poellinger, L. (1995) *J. Biol. Chem.* **270,** 13968–13972
35. Huffman, J. L., Mokashi, A., Bachinger, H. P., and Brennan, R. G. (2001) *J. Biol. Chem.* **276,** 40537–40544
36. Jain, S., Maltepe, E., Lu, M. M., Simon, C., and Bradfield, C. A. (1998) *Mech. Dev.* **73,** 117–123
37. Aitola, M. H., and Pelto-Huikko, M. T. (2003) *J. Histochem. Cytochem.* **51,** 41–54
38. Prasch, A. L., Heideman, W., and Peterson, R. E. (2004) *Toxicol. Sci.* **82,** 250–258
39. Pongratz, I., Antonsson, C., Whitelaw, M. L., and Poellinger, L. (1998) *Mol. Cell. Biol.* **18,** 4079–4088
40. Yang, J., Zhang, L., Erbel, P. J., Gardner, K. H., Ding, K., Garcia, J. A., and Bruick, R. K. (2005) *J. Biol. Chem.* **280,** 36047–36054
41. Erbel, P. J., Card, P. B., Karakuzu, O., Bruick, R. K., and Gardner, K. H. (2003) *Proc. Natl. Acad. Sci. U. S. A.* **100,** 15504–15509
42. Card, P. B., Erbel, P. J., and Gardner, K. H. (2005) *J. Mol. Biol.* **353,** 664–677

Xenobiotica, April 2006; 36(4): 301–314

Taylor & Francis
Taylor & Francis Group

Species differences in hydrolase activities toward OT-7100 responsible for different bioavailability in rats, dogs, monkeys and humans

S. KURIBAYASHI[1,2] N. UEDA[2], S. NAITO[2], H. YAMAZAKI[1], & T. KAMATAKI[1]

[1]*Division of Drug Metabolism, Graduate School of Pharmaceutical Sciences, Hokkaido University, Sapporo, Japan and* [2]*Division of Pharmacology, Drug Safety and Metabolism, Otsuka Pharmaceutical Factory, Inc., Tokushima, Japan*

(Received 16 September 2005)

Abstract

OT-7100 (5-*n*-butyl-7-(3,4,5-trimethoxybenzoylamino)pyrazolo[1,5-a] pyrimidine) is an amide moiety-bearing pyrazolopyrimidine derivative with a potential analgesic effect. To determine the factors responsible for observed species differences in the bioavailability of this drug, human and experimental animal samples were used to investigate *in vitro* microsomal and cytosolic hydrolase activities in the liver and small intestine vis-à-vis the pharmacokinetics of OT-7100. The AUC_{0-t} values of OT-7100 after oral administration in rats, dogs and monkeys were 0.163, 0.0383 and 0.00147 $\mu g\,h\,ml^{-1}$ divided by $mg\,kg^{-1}$, respectively. The bioavailabilities of OT-7100 after oral administration in rats, dogs and monkeys were 36, 17 and 0.3%, respectively. The plasma concentration–time profiles of intravenously administrated OT-7100 in rats, dogs and monkeys were similar. The hydrolase activities toward OT-7100 in liver microsomes or cytosol were approximately similar in rats, dogs, monkeys and humans. In contrast, hydrolase activities of small intestinal microsomes from monkeys were higher (36.1 $ng\,mg\,protein^{-1}\,min^{-1}$) than those of rats, dogs and humans (5.4, 1.4 and 4.3 $ng\,mg\,protein^{-1}\,min^{-1}$, respectively). These results suggest that the primary factor influencing first-pass metabolism for the OT-7100 is enzymatic hydrolysis in the small intestine. This information provides an important index for extrapolating the pharmacokinetics of drugs in humans using studies on monkeys.

Keywords: *Species differences, pyrazolopyrimidine derivative, hydrolysis, bioavailability, small intestine*

Correspondence: S. Kuribayashi, Department of Drug Metabolism, Division of Pharmacology, Drug Safety and Metabolism, Otsuka Pharmaceutical Factory Inc., 115 Tateiwa, Muya-cho, Naruto, Tokushima 772-8601, Japan. Tel: 81-88-685-1151. Fax: 81-88-686-8176. E-mail: kuribasy@otsukakj.co.jp

ISSN 0049-8254 print/ISSN 1366-5928 online
DOI: 10.1080/00498250600571798

Introduction

In vivo preclinical pharmacokinetic studies are a key component of the overall drug discovery and development paradigm. Typically for a given drug candidate, pharmacokinetic data are first available in at least two or three preclinical species, often including rat, dog and/or monkey, well before clinical data emerge. In practice, however, species differences often complicate extrapolation of preclinical species data to the predicted pharmacokinetics of a molecule in humans (Boxenbaum 1980; Lin 1995). It is widely accepted that the liver is the primary site of first-pass metabolism because of both its size and high content of drug-metabolizing enzymes (Thummel et al. 1997). However, it is gradually becoming evident that metabolizing enzymes involved in the process of absorption in the small intestine also play a crucial role, in some cases, in metabolizing drugs delivered orally (Satoh and Hosokawa 1998; Lin et al. 1999). For example, both hepatic and intestinal enzymes have been implicated in the first-pass metabolism of midazolam after oral administration (Thummel et al. 1996). Differences between humans and experimental animals in the bioavailability of an active metabolite from glycovir arose from differences in the hydrolysis rate of glycovir within the small intestinal mucosa (Cook et al. 1995). Furthermore, there is insufficient predictive accuracy in scale-up estimation even when results from drug studies in monkeys are used to extrapolate to humans (Inaba et al. 1998). Therefore, it is important to investigate species differences/similarities with respect to intestinal drug-metabolizing enzymes in humans and experimental animals in order to improve one's understanding of bioavailability.

Drug-metabolizing enzymes such as cytochrome P450 (CYP) (Zhang et al. 1999; Hashizume et al. 2001) and carboxylesterases (Campbell et al. 1987; Satoh 1987), which are involved in phase I reactions, are present in high concentrations in the small intestine. Hepatic CYP3A4 has been involved in the oxidative metabolism of many drugs (Fitzsimmons and Collins 1997). In contrast, carboxylesterases are important for the hydrolysis of many exogenous compounds, resulting in both activation of prodrugs and inactivation of drugs (Hosokawa et al. 1995; Satoh and Hosokawa 1998). Marked interspecies variations in carboxylesterase activity exist in the small intestine and liver, and there are significant differences in substrate specificity of the various carboxylesterase isoforms (Inoue et al. 1979; Hosokawa et al. 1990). However, since this has not been systematically studied based on chemical structure, there is little information about species differences/similarities between human and monkey carboxylesterases. Therefore, it is difficult to predict the metabolism and pharmacokinetics of drugs in humans based on animal studies.

OT-7100 (5-*n*-butyl-7-(3,4,5-trimethoxybenzoylamino)pyrazolo[1,5-a] pyrimidine) is a pyrazolopyrimidine derivative with the amide moiety that has a potential analgesic effect (Yasuda et al. 1999, 2001; Miki et al. 2001). The proposed metabolic pathways of OT-7100 in rats and dogs are shown in Figure 1.

The metabolites of OT-7100 included M19 and M5, which are hydrolysate of the amide moiety of OT-7100, and M1–3, which result from oxidization of the *n*-butyl groups by CYPs (unpublished data). It is believed that the hydrolysis of OT-7100 is responsible for the species differences and that hydrolysis influences the pharmacokinetics and biotransformation of OT-7100, as well as other drugs with the amide moiety (Satoh and Hosokawa 1998). Since the small intestinal carboxylesterases apparently play an important role in the metabolism and biotransformation of orally administered drugs, it is important to investigate the species differences in the hydrolase activity between humans and experimental animals and to identify the contribution of small intestine

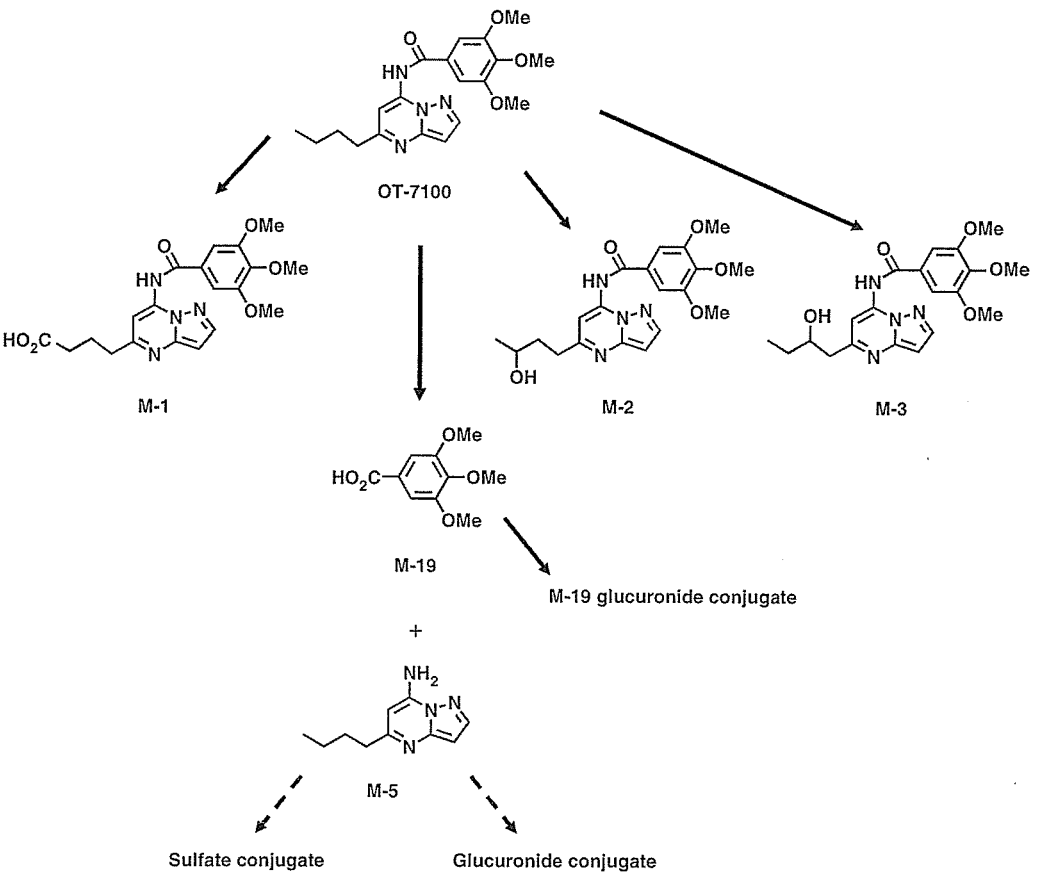

Figure 1. Postulated metabolic pathways of OT-7100 in rats and dogs.

metabolism to the total hydrolysis fraction of an orally administered drug containing the amide moiety.

The present study reports that the different bioavailabilities of the orally administered probe drug OT-7100 with an amide moiety could be accounted for by the differences in specific small intestinal hydrolase activities among humans and experimental animals (rats, dogs and monkeys). It was found that OT-7100 is a good substrate to identify species differences in small intestinal hydrolase activities, particularly between humans and monkeys. The authors have demonstrated that hydrolase activity in the small intestine is one of the primary drug metabolism factors influencing first-pass metabolism in the process of drug absorption.

Materials and methods

Materials

OT-7100 (5-*n*-butyl-7-(3,4,5-trimethoxybenzoylamino)pyrazolo[1,5-a] pyrimidine; molecular weight of 384.44; Figure 1) and its five metabolites (M1–3, M5 and M19) were synthesized at Otsuka Pharmaceutical Factory (Tokushima, Japan). All chemicals

were determined, by reversed-phase HPLC, to be >99.0% pure. All other chemicals and reagents used were of analytical reagent grade.

Animals

Male Sprague–Dawley rats, 6–7 weeks of age, weighing 190–250 g (Charles River Japan, Kanagawa, Japan) and male Beagle dogs, 11–12 months of age, weighing 10.10–10.78 kg (LRE-Strain, HRP, Inc., Kalamazoo, MI, USA) were used. The animals were housed in a room maintained at 23 ± 3°C and at a relative humidity of 55% ± 15%, with an air exchange rate of at least 10 times h^{-1} and a 12-h light/dark cycle. Male cynomolgus monkeys, 3 years of age, weighing approximately 3 kg, were individually housed at the Wakayama Breeding Farm of Keari Co. Ltd (Wakayama, Japan) at 22–26°C and a relative humidity of 45–65%. Animals were fed solid diet (rat; CRF-1, dog; DS-5, monkey; PS, Oriental Yeast Co. Ltd, Tokyo, Japan) once daily and allowed free access to tap water. These studies were approved by the Committee on the Care and Use of Laboratory Animals for the Otsuka Pharmaceutical Factory, Inc, and we followed guidelines similar to those provided in the Guide for the Care and Use of Laboratory Animals (National Research Council, USA).

Preparation of subcellular fractions

Dog, monkey and human liver microsomes and cytosol from three individuals were purchased from KAC Corp (Kyoto, Japan). Rat liver microsomes and cytosol were prepared from three animals. Male rats (Sprague–Dawley, 7 weeks old) were purchased from Charles River Japan. A 3 × volume 0.15 M KCl containing 10 mM EDTA 2Na (adjusted at pH 7.4 using 0.15 M KOH and 0.15 M HCl) was added to the liver and homogenized in an ice bath. The homogenate was centrifuged at 9000*g* for 20 min at 4°C, and an aliquot of the supernatant was further centrifuged at 105 000*g* for 60 min at 4°C. The supernatant, cytosol, was stored at −80°C until use. The remaining pellet fractions were collected, suspended again with 10 ml 100 mM potassium phosphate buffer (pH 7.4) containing 20% glycerol and 1 mM EDTA 2Na, and stored at −80°C until use.

Dog, monkey and human small intestinal microsomes and cytosol from three individuals were purchased from KAC Corp (Kyoto, Japan). One lot of rat small intestinal microsomes and cytosol were prepared from five animals. Male rats (Sprague–Dawley, 7 weeks old) were purchased from Charles River Japan. The small intestine was collected and the inner-side of small intestine was washed with 50 ml ice-cold physiological salt solution. The residual washing solution was then removed from outside the small intestine. The small intestine was incised and the mucosa was then collected from the inner-side by scrapping using a slide-glass. The small intestinal mucosa from five rats were pooled and weighed. A 3 × volume of 0.15 M KCl (adjusted at pH 7.4 using 0.15 M KOH and 0.15 M HCl) containing 10 mM EDTA 2Na and trypsin inhibitor (0.5 mg ml^{-1}) was added to the small intestinal mucosa and homogenized in an ice bath. The homogenate was centrifuged at 9000*g* for 20 min at 4°C, and an aliquot of the supernatant was further centrifuged at 105 000*g* for 60 min at 4°C. The supernatant, cytosol, was stored at −80°C until use. The remaining pellet fractions were collected, suspended again with 2 ml 100 mM potassium phosphate buffer (pH 7.4) containing trypsin inhibitor (0.5 mg ml^{-1}) and 1 mM EDTA 2Na, and stored at −80°C until use. Proteins were determined by the method of Lowry et al. (1951), with bovine serum albumin as a standard.